

1   **Title:** Gene flow influences the genomic architecture of local adaptation in six riverine fish  
2   species

3   **Running Title:** Gene flow influences genomic architecture of local adaptation

4   **Authors:** Yue Shi<sup>1,2,\*</sup>, Kristen L. Bouska<sup>3</sup>, Garrett J. McKinney<sup>4</sup>, William Dokai<sup>1,2</sup>, Andrew  
5   Bartels<sup>5</sup>, Megan V. McPhee<sup>1</sup>, Wesley A. Larson<sup>6,7</sup>

6   **Contact information:**

7   <sup>1</sup>College of Fisheries and Ocean Sciences, University of Alaska Fairbanks, 17101 Point Lena  
8   Loop Road, Juneau, AK 99801, USA.

9   <sup>2</sup>Wisconsin Cooperative Fishery Research Unit, College of Natural Resources, University of  
10   Wisconsin-Stevens Point, 800 Reserve St., Stevens Point, WI 54481, USA.

11   <sup>3</sup>U.S. Geological Survey, Upper Midwest Environmental Sciences Center, 2630 Fanta Reed  
12   Road, La Crosse, WI 54603, USA.

13   <sup>4</sup>NRC Research Associateship Program, Northwest Fisheries Science Center, National Marine  
14   Fisheries Service, National Oceanic and Atmospheric Administration, 2725 Montlake Blvd E,  
15   Seattle, WA 98112, USA.

16   <sup>5</sup>Long Term Resource Monitoring Program, Wisconsin Department of Natural Resources, 2630  
17   Fanta Reed Road, La Crosse, WI 54603, USA.

18 <sup>6</sup>National Oceanographic and Atmospheric Administration, National Marine Fisheries Service,  
19 Alaska Fisheries Science Center, Auke Bay Laboratories, 17109 Point Lena Loop Road, Juneau,  
20 AK 99801, USA

21 <sup>7</sup>U.S. Geological Survey, Wisconsin Cooperative Fishery Research Unit, College of Natural  
22 Resources, University of Wisconsin-Stevens Point, 800 Reserve St., Stevens Point, WI 54481,  
23 USA

24 \*Corresponding author. Email address: [yshi8@alaska.edu](mailto:yshi8@alaska.edu)

25 **Abstract**

26 Understanding how gene flow influences adaptive divergence is important for predicting  
27 adaptive responses. Theoretical studies suggest that when gene flow is high, clustering of  
28 adaptive genes in fewer genomic regions would protect adaptive alleles from among-population  
29 recombination and thus be selected for, but few studies have tested this hypothesis with  
30 empirical data. Here, we used RADseq to generate genomic data for six fish species with  
31 contrasting life histories from six reaches of the Upper Mississippi River System, USA. We then  
32 conducted genome scans for genomic islands of divergence to examine the distribution of  
33 adaptive loci and investigated whether these loci were found in inversions. We found that gene  
34 flow varied among species, and adaptive loci were clustered more tightly in species with higher  
35 gene flow. For example, the two species with the highest overall  $F_{ST}$  (0.03 - 0.07) and therefore  
36 lowest gene flow showed little evidence of clusters of adaptive loci, with adaptive loci spread  
37 uniformly across the genome. In contrast, nearly all adaptive loci in the species with the lowest  
38  $F_{ST}$  (0.0004) were found in a single large putative inversion. Two other species with intermediate  
39 gene flow ( $F_{ST} \sim 0.004$ ) also showed clustered genomic architectures, with most islands of  
40 divergence clustered on a few chromosomes. These results provide important empirical evidence  
41 to support the hypothesis that increasingly clustered architectures of local adaptation are  
42 associated with high gene flow. Our study utilized a unique system with species spanning a large  
43 gradient of life histories to highlight the importance of gene flow in shaping adaptive divergence.

44 **Keywords:** Freshwater fishes, local adaptation, gene flow, genomic islands of divergence,  
45 chromosomal inversions, Mississippi River

47 **Introduction**

48 Understanding the genomic basis of adaptation is a central goal of evolutionary biology.  
49 Research on this topic largely focuses on identifying genetic markers involved in adaptation and  
50 assessing the distribution of these markers across the genome (Narum & Hess 2011; Yeaman  
51 2013; Lotterhos & Whitlock 2014; Hoban *et al.* 2016; Forester *et al.* 2018). Substantial efforts  
52 have focused on this area of research for decades (Smith & Haigh 1974; Rieseberg 2001; Noor *et*  
53 *al.* 2001). However, results have been highly variable across taxa and systems, making it difficult  
54 to gain a mechanistic understanding of the evolutionary processes that influence the genomic  
55 landscape of adaptation. For example, many studies have found that alleles contributing to local  
56 adaptation tend to be clustered together in genomic islands of differentiation, while other studies  
57 have found little or no evidence of adaptive alleles clustering within genomic islands (Nosil *et al.*  
58 2009; Strasburg *et al.* 2012; Roda *et al.* 2017; Johannesson *et al.* 2020; Thompson *et al.* 2020).  
59 This mixed evidence raises an important evolutionary question: when are loci affecting adaptive  
60 divergence expected to be tightly clustered?

61 Interpreting results from genome scans in the context of gene flow may aid in the understanding  
62 of genomic landscapes of adaptation (Marques *et al.* 2016). Gene flow can be beneficial for  
63 maintaining population connectivity and genetic diversity by introducing novel genetic variation  
64 but it can also impede local adaptation by introducing maladaptive foreign alleles into a locally  
65 adapted populations (Bolnick & Nosil 2007). One potential evolutionary ‘solution’ that may  
66 minimize maladaptive effects of gene flow is for selection to favor clustered architectures of  
67 adaptation, where adaptive alleles are tightly linked and locally favorable combinations of alleles  
68 are protected from disruption via low recombination (Yeaman 2013; Roesti 2018).

69 Several mechanisms have been proposed to explain the observations of clustered genomic  
70 architectures of adaptive alleles when gene flow is high, including divergence hitchhiking and  
71 the utilization of genomic rearrangements to protect adaptive loci from recombination.  
72 Divergence hitchhiking occurs when gene exchange between diverging populations is reduced  
73 around a gene under strong divergent selection (Via 2012). This process can produce islands of  
74 differentiation spanning multiple megabases, as free recombination among populations is  
75 reduced due to assortative mating (Via 2012). Genomic rearrangements, such as chromosomal  
76 inversions, can also facilitate adaptation in the face of high gene flow and lead to genomic  
77 islands of differentiation (Hoffmann & Rieseberg 2008; Yeaman 2013; Tigano & Friesen 2016;  
78 Roesti 2018; Wellenreuther & Bernatchez 2018; Aguirre Liguori *et al.* 2019; Huang *et al.* 2020;  
79 Cayuela *et al.* 2020). Inversions are generally not deleterious and do not impact gene function  
80 unless the inversion breakpoint occurs within a gene (Faria *et al.* 2019). However, recombination  
81 between inverted and noninverted arrangements is rare as recombinant gametes are generally  
82 inviable (Huang & Rieseberg 2020). Therefore, if an inversion isolates multiple adaptive alleles,  
83 this architecture will likely be favored, because co-adapted genotypes will be protected from  
84 recombination and allowed to evolve independently even in high gene flow environments  
85 (Rogers *et al.* 2013; Yeaman 2013).

86 Although the theories described above posit that the rate of evolution towards clustered  
87 architectures of local adaptation should increase with gene flow, this hypothesis has largely been  
88 tested with simulations rather than empirical data. For example, Yeaman & Whitlock (2011)  
89 used simulations to demonstrate increasing migration rate, or  $m$ , leads to increasingly  
90 concentrated genomic architectures of adaptation. However, when  $m$  is too high, adaptive  
91 divergence is unlikely because frequent migration prevents even a perfectly adapted mutation

92 from overcoming the homogenizing effects of gene flow. A subsequent simulation study  
93 (Yeaman 2013) highlighted that genomic rearrangement may often be an important component  
94 of local adaptation and when genomic rearrangements are present, tight clustering of adaptive  
95 loci can readily evolve even with high  $m$ .

96 In this study, we investigate how gene flow influences the genomic architecture of adaptation  
97 using genomic data from six riverine fish species that encompass a diverse suite of life histories  
98 and dispersal potentials (Figure 1B). These fish were sampled from the same sites in the Upper  
99 Mississippi River System (UMRS) in the midwestern United States. The UMRS is an  
100 interconnected large river system that hosts a diversity of aquatic habitats in terms of temperature,  
101 turbidity, productivity and flow (Figure 1A & C). Our study system provides a unique  
102 opportunity to compare the genomic architecture of local adaptation in a natural environment for  
103 species with contrasting life histories and assess the influence of gene flow on genomic  
104 architecture. Specifically, we test the hypothesis that the genomic islands of differentiation are  
105 less frequent but larger for species with relatively high gene flow, whereas genomic islands are  
106 more numerous and dispersed throughout the genome for species with low degrees of gene flow.  
107 Our multi-species approach investigating six species inhabiting the same environments is unique,  
108 as most previous studies have focused on closely related species pairs or ecotypes (Nadeau *et al.*  
109 2012; Renaut *et al.* 2012) rather than divergent species inhabiting the same environments.

110 **Materials and Methods**

111 ***Study Design and Genotyping***

112 We collected genetic samples from six fish species found in the UMRS which are native to and  
113 commonly found in the region and have not been extensively stocked: Bullhead Minnow  
114 (*Pimephales vigilax*), Bluegill (*Lepomis macrochirus*), Freshwater Drum (*Aplodinotus*  
115 *grunniens*), Channel Catfish (*Ictalurus punctatus*), Gizzard Shad (*Dorosoma cepedianum*), and  
116 Emerald Shiner (*Notropis atherinoides*). The UMRS is congressionally defined as the  
117 commercially navigable portions of the Mississippi River main stem north of Cairo, Illinois" and  
118 commercially navigable tributaries, including the entire Illinois River (Water Resources  
119 Development Act of 1986, 33 U.S.C. §§ 652). Fin-clip samples were collected from adult fish in  
120 summer 2018 and 2019 across six river reaches (Figure 1A); five of the study reaches are  
121 navigation pools, named for their downstream lock and dam, and the other study reach (Open  
122 River Reach) is an unobstructed, channelized reach. We targeted a sample size of at least 48  
123 samples per species per reach. Samples were genotyped at thousands of SNPs using restriction  
124 site-associated DNA (RAD) sequencing (see Supplementary Methods). Data on life history traits  
125 for each species, including exploitation status, feeding guild, habitat guild, reproductive guild,  
126 spawning migration, and total length were summarized in Table S1. We also obtained data for 20  
127 environmental variables across the six river reaches (Table S2).

128 ***Identification of GEA Outliers and Putatively Neutral SNPs***

129 Recent studies have suggested that genotype-environment association (GEA) methods are more  
130 robust for identifying adaptive loci than traditional differentiation-based methods (Rellstab *et al.*  
131 2015; Forester *et al.* 2018). Differentiation-based outlier tests identify loci with high  $F_{ST}$  values,  
132 which are expected for loci involved in hard selective sweeps with large changes in allele  
133 frequencies (Brauer *et al.* 2016; Forester *et al.* 2018). By comparison, GEA analyses identify

134 genetic variants associated with particular environmental factors and can identify loci under  
135 polygenic and “soft” selective sweeps with relatively small changes in allele frequencies,  
136 providing a more complete view of the genomic landscape of adaptation (Eckert *et al.* 2010;  
137 Brauer *et al.* 2016; Forester *et al.* 2018). For these reasons, we focused on identifying putatively  
138 adaptive loci (henceforth “adaptive loci”) using three GEA methods: redundancy analysis, latent  
139 factor mixed models, and a Bayesian method (Bayenv2). Details of these methods can be found  
140 in the Supplementary Methods. Prior to all three GEA analyses, we conducted principal  
141 component analysis (PCA) on 20 standardized environmental variables. Based on Kaiser-  
142 Guttman criterion and the broken stick model, we retained the first two significant PCs as  
143 environmental composite variables in order to remove collinearity among variables (Figure S1A).  
144 Variables related to temperature, turbidity, pH, and dissolved oxygen had high loadings on  
145 environmental PC1 (Figure S1B), whereas productivity and flow-related variables contributed  
146 significantly to environmental PC2 (Figure S1C). We defined putatively adaptive SNPs as the  
147 GEA outliers (henceforth “GEA outliers”) identified by at least two GEA methods. To determine  
148 which environmental PC that each GEA outlier was most strongly correlated with, we compared  
149 correlation coefficients between each environmental PC and genotype for each outlier using R  
150 function *cor* and assessed which environmental PC had the highest correlation coefficient.

151 To identify datasets of putatively neutral SNPs (henceforth “neutral SNPs”) for each species, we  
152 combined results from GEA analyses with results from additional differentiation-based outlier  
153 tests. While differentiation-based outlier tests may produce a large number of false positives,  
154 they are still useful for conservatively identifying neutral SNPs (Holderegger *et al.* 2006).  
155 Therefore, we ran Bayescan, Arlequin, OutFLANK and *pcadapt* on each species (see

156   Supplementary Methods for details). We defined neutral SNPs as those that were not identified  
157   as outliers by any of the aforementioned seven methods.

158   ***Neutral Genetic Differentiation***

159   We used three methods to estimate population structure for each species with their neutral  
160   datasets. First, we calculated global  $F_{ST}$  ( $F_{ST}$  corrected for sampling bias) using the function  
161   *basic.stats* in *hierfstat* v.0.04-22 (Goudet 2005). Next, we calculated  $F_{ST}$  between all pairs of  
162   river reaches using *genet.dist* function (method="WC84") in *hierfstat*. Significance was assessed  
163   by calculating 95% confidence interval of pairwise  $F_{ST}$  values using *boot.ppfst* function  
164   (nboot=1000) in *hierfstat*. A pairwise  $F_{ST}$  value was considered significant if its confidence  
165   interval did not include zero. Lastly, we conducted PCA implemented in the R package *adegenet*  
166   v2.1.2 (Jombart 2008) to investigate genetic differentiation among individuals.

167   ***Genome Scans for Genomic Islands of Differentiation***

168   We aligned SNPs to reference genomes and conducted genome scans to investigate the genomic  
169   landscape of adaptive divergence. Channel Catfish is the only species with a high-quality  
170   reference genome available in our study. For the other five species, we used high-quality  
171   reference genomes (chromosome-level assemblies) from closely related species (Table S3).  
172   Sequences of filtered RAD loci were mapped to reference genomes with BWA-MEM v 0.7.17  
173   using default settings (Li 2013). We retained sequences with mapping quality > 20 and removed  
174   sequences with "SA:Z" (chimeric alignment) and "XA:Z" tags (alternative hits) using *SAMtools*  
175   v1.10 (Li *et al.* 2009).

176 To identify genomic islands of differentiation, we first calculated F<sub>ST</sub> per locus using the  
177 *basic.stats* function in *hierfstat* for all aligned SNPs across genomes. We then used a Hidden  
178 Markov Model (HMM) approach implemented in the R package *HiddenMarkov* v.1.8-11 (Hofer  
179 *et al.* 2012) to assign each SNP to one of three underlying states, “genomic background”,  
180 “regions of high differentiation” and “regions of low differentiation” based on their F<sub>ST</sub> values,  
181 following the methods detailed in Marques *et al.* (2016). Each of these identified regions can  
182 consist of one or many consecutive SNPs depending on the landscape of differentiation.

183 The HMM approach identified a large number of highly differentiated regions (i.e., genomic  
184 islands of differentiation), but many did not show especially high levels of differentiation and  
185 may be false positives. Therefore, we chose to retain only the genomic islands that contained at  
186 least one differentiation outlier SNP identified by Bayescan, Arlequin or OutFLANK. We  
187 excluded outliers identified only by *pcaadpt* because we discovered this method identified a  
188 much higher number of outliers compared to other methods, which could potentially increase  
189 false positive rate for island detection. We removed genomic islands in situations where a  
190 chromosome only had one island and this island had only one SNP. We also removed islands  
191 located on unplaced scaffolds.

192 ***Identification and Analysis of Putative Inversions***

193 To identify putative inversions, we conducted a sliding window analysis of population structure  
194 across genomes using the R package *lostruct* (Li & Ralph 2019) following the methods described  
195 in Huang *et al.* (2020). We replaced missing genotypes with the most frequent genotype and  
196 divided each genome into nonoverlapping windows of either 20 or 50 SNPs depending on the  
197 total number of aligned SNPs for each species. We then used a 40-dimension space

198 multidimensional scaling (MDS) analysis to measure the differences in population structure  
199 patterns among windows, and we defined outlier windows as those with absolute values of  
200 loadings greater than 4 standard deviations above the mean averaged across all windows in the  
201 genome (Huang *et al.* 2020). Outlier windows (single or consecutive) were candidate regions for  
202 putative inversions. We also conducted three additional analyses on putative inversion regions to  
203 provide additional evidence of inversions as suggested by Huang *et al.* (2020). First, because  
204 inversions only suppress recombination in heterozygotes, three distinct genotypic clusters (0, 1, 2)  
205 should be detected along PC1 using PCA, with the outside clusters (0 and 2) representing two  
206 homozygous groups for alternative orientations and the middle cluster (1) representing the  
207 heterozygous group between inversion haplotypes (McKinney *et al.* 2020). The discreteness of  
208 the clustering was calculated as the proportion of the between-cluster sum of squares over the  
209 total using the R function *kmeans* in *adegenet*. Second, we compared heterozygosity (the  
210 proportion of heterozygotes) among three clusters identified by PCA using Wilcoxon tests ( $\alpha =$   
211 0.05) to further confirm the middle group had significantly higher heterozygosity. Finally, we  
212 calculated linkage disequilibrium, or LD ( $r^2$ ) using PLINK v1.9 (Purcell *et al.* 2007; Chang *et al.*  
213 2015) for SNPs with MAF > 0.01 on chromosomes with outlier windows and compared  $r^2$  with  
214 all samples to  $r^2$  calculated only from samples that were homozygous for the most common  
215 orientation. Since inversions are expected to only suppress recombination in heterokaryotypes,  
216 recombination in homokaryotypes should be unaffected.

217 We considered a region as a putative inversion only if all of the following criteria were met: (1) a  
218 distinct three-cluster PCA pattern with discreteness > 0.9; (2) significantly elevated  
219 heterozygosity in the middle PCA cluster compared to the other two clusters; and (3) elevated  
220 LD calculated with all samples, but not with homozygous samples. We assumed that the more

221 derived inversion arrangement would have lower heterozygosity given its relatively recent origin  
222 compared to the ancestral state (Laayouni 2003; Twyford & Friedman 2015; Knief *et al.* 2016).  
223 Notably, when examining our data, we found five additional regions with discreteness very close  
224 to 0.9 (0.893 - 0.898) that displayed distinct three-cluster PCR patterns, and we included these  
225 regions as candidates for putative inversions as well.

226 To investigate patterns of population structure at putative inversions, we calculated genotype  
227 frequencies in each river reach for each putative inversion. Additionally, we conducted PCA  
228 analyses using all SNPs that were successfully aligned to genomes, SNPs within the identified  
229 inversions, and the remaining aligned SNPs after the SNPs in putative inversions were removed  
230 to compare patterns of genetic structure inferred from datasets including and not including  
231 putative inversions.

### 232 ***Identification and Analyses of Large Clusters of Adaptive Loci***

233 Adaptive loci can be found across many areas of the genome or can be concentrated (i.e.,  
234 clustered) in only a few genomic regions. To determine whether the genomes of our species  
235 contained clustered architectures of adaptative loci, we investigated the distribution of GEA  
236 outliers and islands of differentiation identified by HMM across the genome. We defined  
237 chromosomes exhibiting clustered architecture of adaptation as chromosomes containing at least  
238 3 GEA outliers or 20% of the total HMM islands within a given species. We then calculated the  
239 following genetic metrics to characterize the genomic properties of clustered architectures that  
240 we observed: Fst<sub>pl</sub>, heterozygosity ( $H_O$ ), absolute differentiation ( $D_{xy}$ ), and linkage  
241 disequilibrium (LD).

242 Fst<sub>p</sub> and  $H_O$  were calculated using the *basic.stats* function in *hierfstat* as described previously.

243 Pairwise per-site  $D_{xy}$  was calculated as  $p_1(1 - p_2) + p_2(1 - p_1)$ , where  $p_1$  is the frequency of a  
244 given allele in the first population and  $p_2$  is the frequency of that allele in the second population  
245 (Irwin *et al.* 2016). Allele frequency was estimated using *makefreq* function (missing = “mean”)  
246 in *adegenet*. Overall  $D_{xy}$  was calculated as the mean of all pairwise  $D_{xy}$  values. LD ( $r^2$ ) was  
247 calculated using PLINK v1.9 for SNPs with MAF > 0.01. We included  $D_{xy}$ , an absolute measure  
248 of genetic differentiation, because defining adaptive genomic regions based solely on relative  
249 measures of differentiation, such as Fst<sub>p</sub>, may identify regions resulting from processes other  
250 than adaptation (Cruickshank & Hahn 2014).

251 For each chromosome, we used Wilcoxon tests ( $\alpha = 0.05$ ) to test for significant differences in  
252 genetic metrics between SNPs within the islands and SNPs outside the islands (chromosomal  
253 background). We also visualized differences in these metrics with boxplots. To ensure the  
254 differences we observed in four genetic metrics were not due to island size, we randomly  
255 selected five windows outside of the islands as chromosomal background with window size  
256 (number of SNPs) set as the average size of all HMM islands found on the corresponding  
257 chromosomes. When calculating the average size of the HMM islands, we removed the HMM  
258 islands containing only one SNP to avoid downward biasing the window size of random  
259 windows in the chromosomal background. We also made sure the randomly selected windows  
260 spanned similar distance ( $\pm 10\%$  bp) compared to the average of all HMM islands found on the  
261 same chromosomes.

262 Lastly, we conducted Gene Ontology (GO) enrichment tests to test for functional enrichment of  
263 genes in the HMM islands located within the six chromosomes displaying clustered architecture.

264 We extracted genes within 10 Kb of a SNP for all SNPs located within the islands for all six  
265 chromosomes, except for chromosome 9 in Emerald Shiner. Since all of the HMM islands on  
266 chromosome 9 in Emerald Shiner were clustered inside of the identified inversion and there was  
267 a relatively smaller number of aligned loci, we extracted genes within 20 Kb of a SNP for all  
268 SNPs located within the identified inversion on the chromosome 9 in Emerald Shiner instead.  
269 See Supplementary Materials for detailed methods about GO enrichment tests.

270 **Results**

271 ***Summary of Sequencing, GEA Outliers, and Neutral SNPs***

272 We RAD sequenced a total of 1,712 individuals, ranging from 275 - 288 individuals per species.  
273 RAD sequencing yielded an average of 5,780,907 retained reads per individual (range = 16,799 -  
274 47,250,859). After filtering, 1,417 individuals (179 - 256 individuals per species) were retained  
275 and genotyped at 10,834 - 28,313 polymorphic SNPs depending on the species (Table S3). Out  
276 of these polymorphic SNPs, 0.04 % to 0.3% were identified as GEA outliers, and 95.9 % - 99.4%  
277 were identified as neutral SNPs in each species (Table S4). For most species, the majority of  
278 GEA outliers were found to be strongly associated with environmental PC1 (temperature,  
279 turbidity, pH, and dissolved oxygen related). In contrast, GEA outliers in Freshwater Drum were  
280 strongly associated with environmental PC2 (productivity and flow related) (Table S4).

281 ***Neutral Genetic Differentiation***

282 Patterns of population structure estimated from the neutral datasets spanned a large gradient of  
283 genetic differentiation across species (Figure 2, Table S5). Bullhead Minnow had the highest  
284 global  $F_{ST}$  value of 0.0720 with pairwise  $F_{ST}$  values ranging from 0.0041 to 0.1543, followed by

285 Bluegill (global F<sub>ST</sub> = 0.0302; pairwise F<sub>ST</sub> = 0.0014 - 0.0739), Freshwater Drum (global F<sub>ST</sub> =  
286 0.0050, pairwise F<sub>ST</sub> = -0.0003 - 0.0169), Channel Catfish (global F<sub>ST</sub> = 0.0025, pairwise F<sub>ST</sub> =  
287 0.0003 - 0.0048), and Gizzard Shad (global F<sub>ST</sub> = 0.0024, pairwise F<sub>ST</sub> = 0.0003 - 0.0051).  
288 Emerald Shiner had the lowest global F<sub>ST</sub> value among all six species, 0.0004, with pairwise F<sub>ST</sub>  
289 values ranging from -0.0003 to 0.0016.

290 Results of the PCAs (Figure 3) corroborated the patterns described above. In Bullhead Minnow,  
291 we detected five genetic clusters, with individuals from each river reach forming a single cluster  
292 except for Pool 8 and Pool 13, which were grouped together. In Bluegill, individuals from the  
293 three northern river reaches (Pool 4, Pool 8, and Pool 13) were genetically similar, Pool 26 and  
294 La Grange formed a second cluster, while the most southerly reach, Open River, formed its own  
295 cluster. In Freshwater Drum, individuals from La Grange grouped separately from other  
296 populations along with some individuals from Pool 26 and Open River. In Channel Catfish,  
297 individuals from the Open River were slightly separated from all the other reaches. Lastly,  
298 Gizzard Shad and Emerald Shiner showed no apparent population structure.

299 ***Genome Scan for Genomic Islands of Differentiation***

300 We aligned SNPs to reference genomes and conducted genome scans to investigate the genomic  
301 landscape of adaptive divergence. A total of 3,348 - 16,620 loci were aligned to the  
302 corresponding reference genomes with alignment rate varying from 26.4% to 97.5% depending  
303 on genetic divergence from the reference species (Table S3). Correspondingly, a total of 2 - 25  
304 GEA outliers were aligned with alignment rate per species varying from 25.7% to 100% (Table  
305 S4).

306 Genome scan results revealed highly variable genomic landscapes of population differentiation  
307 among the six species (Figure 2). In general, GEA outliers and HMM islands in species with  
308 lower neutral differentiation were more tightly clustered and found on fewer chromosomes,  
309 whereas those in species with higher neutral differentiation were spread out across the genome.  
310 Bullhead Minnow (highest neutral population structure) displayed a high level of baseline  
311 differentiation without obvious peaks of highly differentiated loci. We only detected 2 islands on  
312 2 chromosomes and there were no GEA outliers located within the islands. In Bluegill, the  
313 species with the second highest neutral population structure, we identified 83 islands that were  
314 dispersed across nearly all chromosomes (22/24) with no chromosomes containing more than 8%  
315 of islands. Additionally, 15 out of 21 aligned GEA outliers (71%) were located in 12 islands  
316 across 9 chromosomes with only 3 islands having more than one GEA outliers (up to 2).  
317 Freshwater Drum had an intermediate level of population differentiation and displayed a more  
318 clustered architecture of genomics islands of differentiation compared to Bullhead Minnow and  
319 Bluegill. In total, 14 islands were detected across 6 chromosomes and no GEA outliers were  
320 found within islands. Of these islands, 3 islands (21%) were clustered on chromosome 7 and 7  
321 islands (50%) were clustered on chromosome 17. Channel Catfish had a relatively low level of  
322 differentiation and displayed highly clustered architectures of adaptation. We identified 15  
323 islands across 10 chromosomes with 3 islands (20%) clustered on chromosome 13. Out of 25  
324 aligned GEA outliers, 6 (24%) were located on an island on chromosome 20 and 4 (16%) were  
325 located on an island on chromosome 28. Gizzard Shad had a similar level of neutral global Fst<sub>p</sub>  
326 as Channel Catfish, but we did not detect any islands of high differentiation, possibly due to its  
327 relatively low genome alignment rate (26.4%). Lastly, Emerald Shiner, the species with lowest  
328 overall neutral population differentiation, displayed the strongest signal of clustered architecture

329 of local adaptation. In Emerald Shiner, 15 islands were detected across 4 chromosomes, of which,  
330 11 (73%) were clustered on chromosome 9. A total of 11 out of 13 aligned GEA outliers (85%)  
331 were found on chromosome 9.

332 ***Identification and Analyses of Putative Inversions***

333 Using local PCA in *lostruct*, we identified 21 candidate regions for putative inversions where  
334 individuals clustered into three distinct groups on PC1 and with the middle PCA cluster  
335 displaying significantly higher heterozygosity than the other two clusters (Table S6). Of all  
336 candidate regions, only the ones on chromosome 14 in Channel Catfish and chromosome 6, 9,  
337 and 19 in Emerald Shiner were characterized by elevated LD blocks extending over several Mb,  
338 while LD decayed very quickly on other chromosomes (Figure S2). However, we detected  
339 recombination suppression in both heterozygous and homozygous groups in the outlier region on  
340 chromosome 14 in Channel Catfish (Figure S3). This pattern is inconsistent with the theory that  
341 inversions should only suppress recombination in heterokaryotypes, so this region was excluded.  
342 Only the candidate regions on chromosome 6 (Figure S4), 9 (Figure 4), and 19 (Figure S5) in  
343 Emerald Shiner passed our stringent criteria and were considered as putative inversions. These  
344 three putative inversions spanned large genomic regions, 18.0, 42.7, and 25.6 Mbp, respectively  
345 (Table S6). The two homokaryotypes presented significant differences in heterozygosity for all  
346 three putative inversions (Figure 4B, S5B and S6B) and we assumed that the arrangement with  
347 lower heterozygosity was the derived inverted type. The putative inversion on chromosome 9  
348 (cluster 0) was only detected in the three southern river reaches (Figure 4C), whereas the other  
349 two inversions occurred at similar frequency across all six river reaches, ranging in frequencies  
350 from 0.15 to 0.39 for the inversion on chromosome 6 (cluster 2; Figure S4C), and from 0.19 to

351 0.28 for the inversion on chromosome 19 (cluster 0; Figure S5C). Moreover, GEA outliers and  
352 HMM islands were consistently associated with the putative inversion on chromosome 9 in  
353 Emerald Shiner (Figure 2). However, no GEA outliers or HMM islands were found within the  
354 inversions on the chromosome 6 and 19.

355 Analyzing datasets with and without putative inversions in Emerald Shiner produced  
356 substantially different patterns of genetic structure (Figure 5). Both PCA analyses based on all  
357 aligned SNPs and SNPs within the three identified inversions showed a similar genetic structure  
358 pattern, with six well-separated clusters. This illustrates that the clustering inferred from the full  
359 dataset is driven by these three inversions. After the SNPs in these inversions were removed, the  
360 remaining aligned loci demonstrated a lack of clustering, with panmictic population structure.

361 ***Genomic Properties of Large Clusters of Adaptive Loci***

362 The following chromosomes exhibited highly clustered architecture with at least 3 GEA outliers  
363 or 20% HMM islands within a given species: (1) chromosome 7 and 17 in Freshwater Drum; (2)  
364 chromosome 13, 20, and 28 in Channel Catfish; and (3) chromosome 9 in Emerald Shiner  
365 (Figure 2). The HMM islands on most of these chromosomes were characterized by high  
366 population differentiation and co-located with several GEA outliers strongly associated with  
367 environmental variables except for Freshwater Drum, where no GEA outliers were found within  
368 clusters of HMM islands. In all six chromosomes with clustered architectures we found, as  
369 expected, significantly higher  $F_{ST}$  values within the HMM islands (Figure 6). Comparisons of  
370  $H_O$  and  $D_{xy}$  between HMM islands and chromosomal background showed three different patterns  
371 among six chromosomes: (1) islands on chromosome 7 and 17 in Freshwater Drum and  
372 chromosome 9 in Emerald Shiner had similar  $H_O$  and  $D_{xy}$ ; (2) islands on chromosome 13 in

373 Channel Catfish had significantly higher values of  $H_O$  and  $D_{xy}$ ; (3) islands on chromosome 20  
374 and 28 in Channel Catfish had significantly lower values of  $H_O$  and  $D_{xy}$  (Figure 6). We also  
375 found significantly elevated LD within the islands in all chromosomes except for chromosome  
376 13 in Channel Catfish (Figure 6). Taken together, these results indicate that the HMM islands on  
377 the six chromosomes with clustered architectures have higher relative divergence than their  
378 chromosomal backgrounds; the islands on chromosome 13 in Channel Catfish also demonstrated  
379 higher absolute divergence, though without elevated LD.

380 A total of 9, 12, and 2 GO terms were significantly enriched ( $p < 0.05$ ) in the HMM islands on  
381 chromosome 17 in Freshwater Drum, the island on chromosome 28 in Channel Catfish, and the  
382 inversion on chromosome 9 in Emerald Shiner, respectively (Table S7). Enriched GO terms  
383 included regulation of cellular component size, cell communication, and regulation of ion  
384 transmembrane transport. There were no annotated genes found within the HMM island(s) on  
385 chromosome 7 in Freshwater Drum, chromosome 13 and 20 in Channel Catfish.

386 **Discussion**

387 ***Neutral Population Structure Reflects Differences in Life History Strategies Among Species***

388 We found highly variable neutral population structure among our six riverine fish species that  
389 generally reflected differences in life history strategies. For example, both Bullhead Minnow and  
390 Bluegill, which had the highest levels of genetic differentiation, are nest spawners whose eggs  
391 and larvae are not transported by currents, limiting gene flow. In contrast, Gizzard Shad and  
392 Emerald Shiner, which had the lowest levels of structure in our study, are both broadcast  
393 spawners, allowing their eggs to be carried freely by the currents, facilitating gene flow. Genetic

394 studies on similar fish species have generally corroborated the patterns we observed, with nest  
395 spawning species such as smallmouth bass (*Micropterus dolomieu*) exhibiting high levels of  
396 genetic structure in open systems compared to broadcast spawning species such as walleye  
397 (*Sander vitreus*) (Ruzich *et al.* 2019; Euclide *et al.* 2020; 2021)

398 An exception to the pattern described above was Channel Catfish, as they are nest spawners but  
399 displayed relatively low levels of differentiation. It is possible that the highly migratory nature of  
400 this species mixed with potentially low spawning fidelity (Pellett *et al.* 1998) could explain the  
401 low to intermediate levels of population differentiation we observed. Freshwater Drum also  
402 deviated from the expected patterns of population structure based on life history, as they are  
403 migratory broadcast spawners but displayed an intermediate level of population structure, with  
404 individuals from La Grange along with some individuals from southern populations in Pool 26  
405 and Open River forming a distinct group. One possible explanation for this pattern is limited  
406 movement of Freshwater Drum between the Illinois River, where La Grange is located, and the  
407 mainstem Mississippi River. Unfortunately, movement data for this species are generally lacking,  
408 making it difficult to corroborate this hypothesis without additional research.

409 ***GEA Outliers Reflect Adaptive Divergence in Response to Habitat Heterogeneity***

410 Most of the GEA outliers that we found were associated with environmental PC1, which had the  
411 highest loadings for temperature and turbidity. It is likely that these GEA outliers reflect adaptive  
412 divergence driven by the large latitudinal gradient that we sampled. Our study system spans two  
413 major Köppen climate zones, with pools 4, 8, and 13 in a humid continental climate  
414 characterized by warm summers and very cold winters (below 0 °C), and Pool 26, Open River,  
415 and La Grange in a humid subtropical climate characterized by very warm and humid summers

416 and mild winters (above 0 °C). Although we could not disentangle the effects of temperature and  
417 turbidity because they co-varied, we suspect that temperature is likely a major selective force  
418 shaping adaptive divergence in our study system given its pervasive effects across all levels of  
419 biological processes, from the biochemistry of metabolism (Deutsch *et al.* 2015) to reproduction  
420 (Pankhurst & Munday 2011) and the fact that most fish are ectotherms. Multiple studies have  
421 illustrated strong signals of adaptive divergence across temperature gradients in continuously  
422 distributed marine species, even when differentiation at neutral markers is low (Limborg *et al.*  
423 2012; Stanley *et al.* 2018; Wilder *et al.* 2020). However, few studies have investigated  
424 temperature-mediated adaptive divergence in continuously distributed freshwater fish. Our study  
425 suggests riverine fish display patterns of strong adaptive divergence driven by temperature that  
426 are similar to those found in marine systems, highlighting the fact that populations of  
427 continuously distributed riverine species may display the potential for local adaptation across  
428 their range.

429 While GEA outliers for most species in our study were generally associated with environmental  
430 PC1, outliers in Freshwater Drum were associated with environmental PC2, which displayed  
431 high loadings for measures of productivity including chlorophyll and nitrogen, and to a lesser  
432 extent, flow. This result suggests that the environmental variables influencing adaptive  
433 divergence in Freshwater Drum may differ from our other study species. Specifically, it is  
434 possible that Freshwater Drum is more affected by eutrophication caused by agricultural runoff  
435 compared to our other study species. Numerous studies have demonstrated that fish species  
436 respond differently to eutrophication depending on their life histories (Tammi *et al.* 1999;  
437 Hondorp *et al.* 2010; Jacobson *et al.* 2017). Alternatively, Freshwater Drum might have evolved  
438 in response to an underlying geomorphological condition correlated with agricultural inputs or to

439 variation along a lotic-lentic gradient, to which Freshwater Drum are known to respond (Rypel *et*  
440 *al.* 2006; Jacquemin *et al.* 2015).

441 ***Gene Flow Influences the Genomic Architecture of Local Adaptation***

442 Theoretical studies and genetic simulations predict that increased gene flow will lead to  
443 increasingly concentrated genomic architecture of adaptation (Yeaman & Whitlock 2011; Via  
444 2012; Yeaman 2013). However, few empirical studies have tested this hypothesis in natural  
445 populations, and the results of these empirical studies have not necessarily supported theoretical  
446 work (Burri *et al.* 2015; Renaud *et al.* 2019). Our study included six fish species spanning a wide  
447 gradient of genetic differentiation (overall  $F_{ST}$  from 0.0004 – 0.07), indicating highly variable  
448 levels of gene flow. Gene flow appeared to be correlated with the landscape of adaptive  
449 divergence, as species with high gene flow (Emerald Shiner, Channel Catfish and Freshwater  
450 Drum) displayed more clustered architecture of adaptation than low gene flow species (Bullhead  
451 Minnow and Bluegill). Our results are somewhat similar to a recent study which examined  
452 adaptive divergence of four flatfish species across a strong salinity gradient in the Baltic Sea (Le  
453 Moan *et al.* 2019). Specifically, Le Moan *et al.* (2019) found more evidence of clustered  
454 architectures of adaption in species displaying low genetic differentiation compared to those  
455 displaying higher differentiation. However, Le Moan *et al.* (2019) sampled a much smaller  
456 gradient of genetic differentiation (overall  $F_{ST}$  from 0.005 – 0.02) than our study and examining  
457 the effects of gene flow on landscapes of adaptive differentiation was not a central goal of their  
458 study.

459 Though our finding that clustered genomic architectures of adaptation (i.e., genomic islands of  
460 divergence) increase with gene flow is in line with theoretical expectations and the results from

461 Le Moan *et al.* (2019), this finding is inconsistent with other studies positing that islands of  
462 divergence are the result of variation in intrinsic recombination rate rather than the combination  
463 of gene flow and selection (Roesti *et al.* 2012; Renaut *et al.* 2019). In fact, there is considerable  
464 debate over the mechanisms that lead to islands of divergence, with past research suggesting that  
465 these islands can be caused by variation in recombination rates (Roesti *et al.* 2012; Renaut *et al.*  
466 2019), linked selection (Cruickshank & Hahn 2014; Burri *et al.* 2015), divergence hitchhiking  
467 (Via 2012), genomic rearrangements including chromosomal inversions (Rogers *et al.* 2013;  
468 Yeaman 2013), and elevated linkage preserving locally adapted alleles (Yeaman & Whitlock  
469 2011). While the cluster of islands on chromosome 9 in Emerald Shiner appears to be caused by  
470 an inversion (see following section), the mechanisms that created the other islands are less clear.

471 To investigate the genomic mechanisms that created the islands on the remaining five  
472 chromosomes exhibiting clustered architecture, we calculated the following four metrics: LD,  
473  $F_{ST}$ ,  $H_O$ , and  $D_{xy}$ , and compared these metrics between islands and chromosomal background.  
474 While islands on all five chromosomes displayed elevated  $F_{ST}$  as expected, we did observe  
475 differences in the remaining three metrics among the chromosomes. Islands on all but one  
476 chromosome displayed elevated LD;  $H_O$  was elevated or similar to neighboring neutral regions in  
477 islands on three out of five chromosomes, and  $D_{xy}$  was elevated or similar to neutral regions in  
478 islands on the same three chromosomes. While LD can be a useful metric for understanding  
479 genomic processes, we found that it did not help us differentiate the mechanisms responsible for  
480 creating islands in the current study and instead focused on  $H_O$  and  $D_{xy}$ . Estimates of  $H_O$  and  $D_{xy}$   
481 suggest that the islands on the two chromosomes with reduced diversity (islands on Channel  
482 Catfish chromosomes 20 and 28) may have been created by linked selection (Cruickshank &  
483 Hahn 2014; Burri *et al.* 2015), while the islands on Channel Catfish chromosome 13 and

484 Freshwater Drum chromosomes 7 and 17 may have arisen through divergent selection (Kulmuni  
485 & Westram 2017).

486 Islands created by divergent selection are hypothesized to have a major role in facilitating  
487 adaptive divergence with gene flow, whereas islands created by linked selection are likely a  
488 result of the underlying genomic landscape and do not necessarily reflect recent adaptive  
489 divergence (Cruickshank & Hahn 2014; Burri *et al.* 2015). Thus, it is extremely important to  
490 differentiate these two types of islands when investigating adaptive divergence. The most  
491 effective way distinguish between these island types is to compare measures of absolute diversity,  
492 as islands created by linked selection should show reduced absolute diversity while islands  
493 created by divergent selection should not (Cruickshank & Hahn 2014; Irwin *et al.* 2016).  
494 Applying this method to our data provided evidence that islands on three of the chromosomes in  
495 our study were created by divergent selection and are likely involved in adaptive divergence with  
496 gene flow whereas the islands on the other two chromosomes were likely a result of ancient  
497 linked selection that acted to reduce diversity in particular genomic regions but is not influencing  
498 contemporary adaptive divergence.

499 Interestingly, we observed variation in the mechanisms putatively responsible for creating  
500 islands both within and among species, as islands on one of the three chromosomes in Channel  
501 Catfish were likely created by divergent selection while islands on the other two chromosomes  
502 were likely the result of linked selection. This result indicates that, while many studies have tried  
503 to generalize the proposed mechanisms responsible for creating islands of divergence, these  
504 mechanisms vary across and even within species (Ottenburghs *et al.* 2020; Liu *et al.* 2020;  
505 Wilder *et al.* 2020). Thus, it is vital to examine both absolute and relative measures of

506 differentiation as well as diversity in newly discovered islands of divergence to help clarify the  
507 mechanisms responsible for creating these islands.

508 ***A Chromosomal Inversion Facilitates Local Adaptation with High Gene Flow in Emerald***  
509 ***Shiner***

510 Our results and those of previous empirical and theoretical studies suggest that divergent  
511 selection can result in clusters of adaptive loci through mechanisms such as divergence  
512 hitchhiking when gene flow is relatively high (Yeaman & Whitlock 2011; Via 2012). However,  
513 when gene flow is extremely high, it is likely that additional genomic mechanisms, such as  
514 structural polymorphisms, may be required to protect clusters of adaptive loci from among-  
515 population recombination caused by gene flow (Yeaman & Whitlock 2011; Rogers *et al.* 2013;  
516 Yeaman 2013; Tigano & Friesen 2016). The gradient of gene flow sampled in our study presents  
517 an excellent opportunity to test this hypothesis. In our study, clustered architectures of adaptation  
518 were common in species with relatively high gene flow, such as Channel Catfish and Freshwater  
519 Drum (average overall  $F_{ST}$  = 0.004), but these clustered architectures did not appear to be  
520 associated with structural polymorphisms. In contrast, in Emerald Shiner, the species with  
521 highest gene flow (overall  $F_{ST}$  = 0.0004), nearly all of the adaptive loci identified were found in  
522 a single genomic region that displayed strong evidence of a chromosomal inversion. Taken  
523 together, our results provide novel empirical evidence to support the theory that chromosomal  
524 inversions are important for facilitating adaptive divergence in systems with extremely high gene  
525 flow.

526 Our study also adds to the growing body of evidence that chromosomal inversions are important  
527 for facilitating adaptive divergence in continuously distributed fish species. Inversions putatively

528 involved in adaptive divergence have been documented in many fishes including Atlantic cod  
529 (*Gadus morhua*) (Kirubakaran *et al.* 2016), lingcod (*Ophiodon elongatus*) (Longo *et al.* 2020),  
530 rainbow trout (*Oncorhynchus mykiss*) (Arostegui *et al.* 2019; Pearse *et al.* 2019), Pacific herring  
531 (*Clupea pallasii*) (Petrou *et al.* 2021), Atlantic silverside (*Menidia menidia*) (Wilder *et al.* 2020),  
532 and European plaice (*Pleuronectes platessa*) (Le Moan *et al.* 2019). However, all of these studies  
533 were conducted on marine fish or salmonids, making our study the first to provide evidence of a  
534 putative adaptive inversion in a non-salmon freshwater fish. It is likely that the lack of previous  
535 evidence for adaptive inversions in freshwater fish is due to the generally higher genetic structure  
536 observed in these species, making inversions less necessary for adaptation. However, our study  
537 illustrates that inversions are likely a larger component of adaptive divergence in freshwater fish  
538 than previously assumed, highlighting the importance of future studies aimed at characterizing  
539 them in additional species.

540 Although inferring the functional significance of the putatively adaptive inversion that we  
541 detected is difficult, it is possible to speculate on its role in facilitating adaptive divergence. The  
542 putatively derived variant of this inversion was only detected in the three southern river reaches  
543 in our study, which are substantially warmer and more turbid than northern reaches. This  
544 suggests that the derived inversion variant may have evolved and increased in frequency as  
545 Emerald Shiner adapted to warmer and/or more turbid environments in more southern regions.  
546 Inversions putatively linked to adaptive divergence across environmental and latitudinal  
547 gradients have also been identified in marine species such as lingcod (Longo *et al.* 2020) and  
548 Atlantic silverside (Wilder *et al.* 2020), but these studies faced similar difficulties when  
549 attempting to describe the functional significance of the adaptive inversions they identified.  
550 Future research combining whole genome resequencing with physiological challenge studies

551 would be useful for assessing the functional role of these inversions in the process of adaptive  
552 divergence.

553 **Conclusions**

554 Our data from six riverine fish species in UMRS displaying a large gradient of life history  
555 strategies suggest that higher gene flow leads to increasingly concentrated genomic architectures  
556 of adaptation. Additionally, our results provide evidence that the mechanisms that create islands  
557 of divergence can be highly variable across and within species, with both ancient linked selection  
558 and more contemporary divergent selection playing important roles in creating genomic islands  
559 of differentiation. Additionally, our study provides further evidence that chromosomal inversions  
560 are important for facilitating adaptive divergence in continuously distributed species with  
561 extremely high gene flow and also sheds light on the documented importance of inversions in  
562 freshwater fish. Taken together, our findings represent a significant contribution towards  
563 understanding the evolutionary processes that influence the genomic landscape of adaptation in  
564 non-model organisms. However, our study used RADseq, which does not assess the full suite of  
565 adaptive divergence across the genome. Future studies should focus on whole genome  
566 resequencing to better understand variation within genomic islands of divergence and to assess  
567 the functional role of these islands in promoting adaptive divergence.

568 **Acknowledgements**

569 This study was funded by the U.S. Army Corps of Engineers Upper Mississippi River  
570 Restoration Program (grant number 96514790661277) and supported by the Turing High  
571 Performance Computing cluster at Old Dominion University. We thank U.S. Geological Survey  
572 Upper Midwest Environmental Sciences Center, Iowa Department of Natural Resources,

573 Minnesota Department of Natural Resources, Wisconsin Department of Natural Resources,  
574 Illinois Natural History Survey, and Missouri Department of Conservation for their great efforts  
575 in sample collection. We thank Kristen Gruenthal for assistance in the laboratory, and Kathi Jo  
576 Jankoswki for help with environmental data access. We are grateful to Uland Thomas for  
577 allowing us to use his fish profile photos of the six study species and Hyeon Jeong Kim for help  
578 with photo editing. Any use of trade, firm, or product names is for descriptive purposes only and  
579 does not imply endorsement by the U.S. Government.

580 **References**

581 Aguirre Liguori JA, Gaut BS, Jaramillo Correa JP *et al.* (2019) Divergence with gene flow is  
582 driven by local adaptation to temperature and soil phosphorus concentration in teosinte  
583 subspecies (*Zea mays parviglumis* and *Zea mays mexicana*). *Molecular Ecology*, **24**, 2663–  
584 17.

585 Arostegui MC, Quinn TP, Seeb LW, Seeb JE, McKinney GJ (2019) Retention of a chromosomal  
586 inversion from an anadromous ancestor provides the genetic basis for alternative freshwater  
587 ecotypes in rainbow trout. *Molecular Ecology*, **28**, 1412–1427.

588 Bolnick DI, Nosil P (2007) Natural selection in populations subject to a migration load.  
589 *Evolution*, **61**, 2229–2243.

590 Brauer CJ, Hammer MP, Beheregaray LB (2016) Riverscape genomics of a threatened fish  
591 across a hydroclimatically heterogeneous river basin. *Molecular Ecology*, **25**, 5093–5113.

592 Burri R, Nater A, Kawakami T *et al.* (2015) Linked selection and recombination rate variation  
593 drive the evolution of the genomic landscape of differentiation across the speciation  
594 continuum of *Ficedula* flycatchers. *Genome Research*, **25**, 1656–1665.

595 Cayuela H, Rougemont Q, Laporte M *et al.* (2020) Shared ancestral polymorphisms and  
596 chromosomal rearrangements as potential drivers of local adaptation in a marine fish.  
597 *Molecular Ecology*, **29**, 2379–2398.

598 Chang CC, Chow CC, Tellier LC *et al.* (2015) Second-generation PLINK: rising to the challenge  
599 of larger and richer datasets. *GigaScience*, **4**, 559–16.

600 Cruickshank TE, Hahn MW (2014) Reanalysis suggests that genomic islands of speciation are  
601 due to reduced diversity, not reduced gene flow. *Molecular Ecology*, **23**, 3133–3157.

602 Deutsch C, Ferrel A, Seibel B, Pörtner H-O, Huey RB (2015) Climate change tightens a  
603 metabolic constraint on marine habitats. *Science*, **348**, 1132–1135.

604 Eckert AJ, van Heerwaarden J, Wegrzyn JL *et al.* (2010) Patterns of population structure and  
605 environmental associations to aridity across the range of Loblolly Pine (*Pinus taeda* L.,  
606 Pinaceae). *Genetics*, **185**, 969–982.

607 Euclide PT, MacDougall T, Robinson JM *et al.* (2021) Mixed-stock analysis using Rapture  
608 genotyping to evaluate stock-specific exploitation of a walleye population despite weak  
609 genetic structure. *Evolutionary Applications*.

610 Euclide PT, Ruzich J, Hansen SP, Zorn TG, Larson WA (2020) Genetic structure of Smallmouth  
611 Bass in the Lake Michigan and Upper Mississippi River drainages relates to habitat, distance,  
612 and drainage boundaries. *Transactions of the American Fisheries Society*, 383–397.

613 Faria R, Johannesson K, Butlin RK, Westram AM (2019) Evolving inversions. *Trends in  
614 Ecology & Evolution*, **34**, 239–248.

615 Forester BR, Lasky JR, Wagner HH, Urban DL (2018) Comparing methods for detecting  
616 multilocus adaptation with multivariate genotype-environment associations. *Molecular  
617 Ecology*, **27**, 2215–2233.

618 Goudet J (2005) HIERFSTAT, a package for R to compute and test hierarchical F-statistics.  
619 *Molecular Ecology Notes*, **5**, 184–186.

620 Hoban S, Kelley JL, Lotterhos KE *et al.* (2016) Finding the genomic basis of local adaptation:  
621 pitfalls, practical solutions, and future directions. *The American Naturalist*, **188**, 379–397.

622 Hofer T, Foll M, Excoffier L (2012) Evolutionary forces shaping genomic islands of population  
623 differentiation in humans. *BMC Genomics*, **13**, 1–13.

624 Hoffmann AA, Rieseberg LH (2008) Revisiting the Impact of Inversions in Evolution: From  
625 Population Genetic Markers to Drivers of Adaptive Shifts and Speciation? *Annual Review of  
626 Ecology, Evolution, and Systematics*, **39**, 21–42.

627 Holderegger R, Kamm U, Gugerli F (2006) Adaptive vs. neutral genetic diversity: implications  
628 for landscape genetics. *Landscape Ecology*, **21**, 797–807.

629 Hondorp DW, Breitburg DL, Davias LA (2010) Eutrophication and fisheries: separating the  
630 effects of nitrogen loads and hypoxia on the pelagic□to□demersal ratio and other measures  
631 of landings composition. *Marine and Coastal Fisheries*, **2**, 339–361.

632 Huang K, Rieseberg LH (2020) Frequency, origins, and evolutionary role of chromosomal  
633 inversions in plants. *Frontiers in Plant Science*, **11**, 1–13.

634 Huang K, Andrew RL, Owens GL, Ostevik KL, Rieseberg LH (2020) Multiple chromosomal  
635 inversions contribute to adaptive divergence of a dune sunflower ecotype. *Molecular  
636 Ecology*, **29**, 2535–2549.

637 Irwin DE, Alcaide M, Delmore KE, Irwin JH, Owens GL (2016) Recurrent selection explains  
638 parallel evolution of genomic regions of high relative but low absolute differentiation in a  
639 ring species. *Molecular Ecology*, **25**, 4488–4507.

640 Jacobson PC, Hansen GJA, Bethke BJ, Cross TK (2017) Disentangling the effects of a century of  
641 eutrophication and climate warming on freshwater lake fish assemblages. *PLoS ONE*, **12**,  
642 e0182667.

643 Jacquemin SJ, Doll JC, Pyron M, Allen M, Owen DAS (2015) Effects of flow regime on growth  
644 rate in freshwater drum, *Aplodonotus grunniens*. *Environmental Biology of Fishes*, 993–1003.

645 Johannesson K, Le Moan A, Perini S, André C (2020) A darwinian laboratory of multiple  
646 contact zones. *Trends in Ecology & Evolution*, 1–16.

647 Jombart T (2008) adegenet: an R package for the multivariate analysis of genetic markers.  
648 *Bioinformatics*, **24**, 1403–1405.

649 Kirubakaran TG, Grove H, Kent MP *et al.* (2016) Two adjacent inversions maintain genomic  
650 differentiation between migratory and stationary ecotypes of Atlantic cod. *Molecular  
651 Ecology*, 2130–2143.

652 Knief U, Hemmrich-Stanisak G, Wittig M *et al.* (2016) Fitness consequences of polymorphic  
653 inversions in the zebra finch genome. *Genome biology*, 1–22.

654 Kulmuni J, Westram AM (2017) Intrinsic incompatibilities evolving as a by-product of  
655 divergent ecological selection: Considering them in empirical studies on divergence with  
656 gene flow. *Molecular Ecology*, 3093–3103.

657 Laayouni H (2003) The evolutionary history of *Drosophila buzzatii*. XXXV. Inversion  
658 polymorphism and nucleotide variability in different regions of the second chromosome.  
659 *Molecular Biology and Evolution*, **20**, 931–944.

660 Le Moan A, Gaggiotti O, Henriques R *et al.* (2019) Beyond parallel evolution: when several  
661 species colonize the same environmental gradient. *bioRxiv*, **26**, 4452–43.

662 Li H (2013) Aligning sequence reads, clone sequences and assembly contigs with BWA-MEM.  
663 *arXiv*, **1303.3887v2**, 1–3.

664 Li H, Ralph P (2019) Local PCA Shows How the Effect of Population Structure Differs Along  
665 the Genome. *Genetics*, **211**, 289–304.

666 Li H, Handsaker B, Wysoker A *et al.* (2009) The sequence alignment/map format and SAMtools.  
667 *Bioinformatics*, **25**, 2078–2079.

668 Limborg MT, Helyar SJ, de Bruyn M *et al.* (2012) Environmental selection on  
669 transcriptome-derived SNPs in a high gene flow marine fish, the Atlantic herring (*Clupea*  
670 *harengus*). *Molecular Ecology*, **21**, 3686–3703.

671 Liu X, Glemin S, Karrenberg S (2020) Evolution of putative barrier loci at an intermediate stage  
672 of speciation with gene flow in campions (*Silene*). *Molecular Ecology*, **11**, 545–15.

673 Longo GC, Lam L, Basnett B *et al.* (2020) Strong population differentiation in lingcod  
674 (*Ophiodon elongatus*) is driven by a small portion of the genome. *Evolutionary Applications*,  
675 2536–2554.

676 Lotterhos KE, Whitlock MC (2014) Evaluation of demographic history and neutral  
677 parameterization on the performance of  $F_{ST}$  outlier tests. *Molecular Ecology*, **23**, 2178–2192.

678 Marques DA, Lucek K, Meier JI *et al.* (2016) Genomics of rapid incipient speciation in  
679 sympatric Threespine Stickleback. *PLoS Genetics*, **12**, e1005887–34.

680 McKinney GJ, Pascal CE, Templin WD *et al.* (2020) Dense SNP panels resolve closely related  
681 Chinook salmon populations. *Canadian Journal of Fisheries and Aquatic Sciences*, **77**, 451–  
682 461.

683 Nadeau NJ, Whibley A, Jones RT *et al.* (2012) Genomic islands of divergence in hybridizing  
684 Heliconius butterflies identified by large-scale targeted sequencing. *Philosophical  
685 Transactions of the Royal Society B: Biological Sciences*, **367**, 343–353.

686 Narum SR, Hess JE (2011) Comparison of  $F_{ST}$  outlier tests for SNP loci under selection.  
687 *Molecular Ecology Resources*, **11**, 184–194.

688 Noor MAF, Grams KL, Bertucci LA, Reiland J (2001) Chromosomal inversions and the  
689 reproductive isolation of species. *Proceedings of the National Academy of Sciences*, **98**,  
690 12084–12088.

691 Nosil P, Funk DJ, Ortiz-Barrientos D (2009) Divergent selection and heterogeneous genomic  
692 divergence. *Molecular Ecology*, **18**, 375–402.

693 Ottenburghs J, Honka J, Müskens GJDM, Ellegren H (2020) Recent introgression between Taiga  
694 Bean Goose and Tundra Bean Goose results in a largely homogeneous landscape of genetic  
695 differentiation. *Heredity*, **125**, 73–84.

696 Pankhurst NW, Munday PL (2011) Effects of climate change on fish reproduction and early life  
697 history stages. *Marine and Freshwater Research*, **62**, 1015–1026.

698 Pearse DE, Barson NJ, Nome T *et al.* (2019) Sex-dependent dominance maintains migration  
699 supergene in rainbow trout. *Nature Ecology & Evolution*, 1–30.

700 Pellett TD, Van Dyck GJ, Adams JV (1998) Seasonal migration and homing of Channel Catfish  
701 in the lower Wisconsin River, Wisconsin. *North American Journal of Fisheries Management*,  
702 85–95.

703 Petrou EL, Fuentes-Pardo AP, Rogers LA *et al.* (2021) Functional genetic diversity in an  
704 exploited marine species and its relevance to fisheries management. *Proceedings of the  
705 Royal Society B: Biological Sciences*, 20202398.

706 Purcell S, Neale B, Todd-Brown K *et al.* (2007) PLINK: a tool set for whole-genome association  
707 and population-based linkage analyses. *The American Journal of Human Genetics*, **81**, 559–  
708 575.

709 Rellstab C, Gugerli F, Eckert AJ, Hancock AM, Holderegger R (2015) A practical guide to  
710 environmental association analysis in landscape genomics. *Molecular Ecology*, **24**, 4348–  
711 4370.

712 Renaut S, Grassa CJ, Yeaman S *et al.* (2019) Genomic islands of divergence are not affected by  
713 geography of speciation in sunflowers. *Nature Communications*, 1–8.

714 Renaut S, Maillet N, Normandeau E *et al.* (2012) Genome-wide patterns of divergence during  
715 speciation: the lake whitefish case study. *Philosophical Transactions of the Royal Society B:  
716 Biological Sciences*, **367**, 354–363.

717 Rieseberg LH (2001) Chromosomal rearrangements and speciation. *Trends in Ecology &  
718 Evolution*, **16**, 351–358.

719 Roda F, Walter GM, Nipper R, Ortiz-Barrientos D (2017) Genomic clustering of adaptive loci  
720 during parallel evolution of an Australian wildflower. *Molecular Ecology*, **26**, 3687–3699.

721 Roesti M (2018) Varied Genomic Responses to Maladaptive Gene Flow and Their Evidence.  
722 *Genes*, **9**, 298–16.

723 Roesti M, Hendry AP, Salzburger W, Berner D (2012) Genome divergence during evolutionary  
724 diversification as revealed in replicate lake-stream stickleback population pairs. *Molecular  
725 Ecology*, **21**, 2852–2862.

726 Rogers SM, Mee JA, Bowles E (2013) The consequences of genomic architecture on ecological  
727 speciation in postglacial fishes. *Current Zoology*, **59**, 53–71.

728 Ruzich J, Turnquist K, Nye N, Rowe D, Larson WA (2019) Isolation by a hydroelectric dam  
729 induces minimal impacts on genetic diversity and population structure in six fish species.  
730 *Conservation Genetics*, **20**, 1421–1436.

731 Rypel AL, Bayne DR, Mitchell JB (2006) Growth of Freshwater Drum from lotic and lentic  
732 habitats in Alabama. *Transactions of the American Fisheries Society*, 987–997.

733 Smith JM, Haigh J (1974) The hitch-hiking effect of a favourable gene. *Genetical Research*, **23**,  
734 23–35.

735 Stanley RRE, DiBacco C, Ben Lowen *et al.* (2018) A climate-associated multispecies cryptic  
736 cline in the northwest Atlantic. *Science Advances*, **4**, eaao929.

737 Strasburg JL, Sherman NA, Wright KM *et al.* (2012) What can patterns of differentiation across  
738 plant genomes tell us about adaptation and speciation? *Philosophical Transactions of the  
739 Royal Society B: Biological Sciences*, **367**, 364–373.

740 Tammi J, Lappalainen A, Mannio J, Rask M, Vuorenmaa J (1999) Effects of eutrophication on  
741 fish and fisheries in Finnish lakes: a survey based on random sampling. *Fisheries  
742 Management and Ecology*, **6**, 173–186.

743 Thompson NF, ANDERSON EC, Clemento AJ *et al.* (2020) A complex phenotype in salmon  
744 controlled by a simple change in migratory timing. *Science*, **609**–613.

745 Tigano A, Friesen VL (2016) Genomics of local adaptation with gene flow. *Molecular Ecology*,  
746 **25**, 2144–2164.

747 Twyford AD, Friedman J (2015) Adaptive divergence in the monkey flower *Mimulus guttatus* is  
748 maintained by a chromosomal inversion. *Evolution*, **69**, 1476–1486.

749 Via S (2012) Divergence hitchhiking and the spread of genomic isolation during ecological  
750 speciation-with-gene-flow. *Philosophical Transactions of the Royal Society B: Biological  
751 Sciences*, **367**, 451–460.

752 Wellenreuther M, Bernatchez L (2018) Eco-evolutionary genomics of chromosomal inversions.  
753 *Trends in Ecology & Evolution*, **33**, 427–440.

754 Wilder AP, Palumbi SR, Conover DO, Therkildsen NO (2020) Footprints of local adaptation  
755 span hundreds of linked genes in the Atlantic silverside genome. *Evolution Letters*, **4**, 430–  
756 443.

757 Yeaman S (2013) Genomic rearrangements and the evolution of clusters of locally adaptive loci.  
758 *Proceedings of the National Academy of Sciences*, **110**, E1743–E1751.

759 Yeaman S, Whitlock MC (2011) The genetic architecture of adaptation under migration-  
760 selection balance. *Evolution*, **65**, 1897–1911.

## 761 **Data Accessibility**

762 Upon acceptance, demultiplexed RAD sequencing data used in this study will be released in the  
763 NCBI with BioProject ID, PRJNA674918. Bioinformatic scripts along intermediate datasets  
764 (post-filtering *vcf*, neutral *vcf*, adaptive *vcf*) supporting this article will be available as a Github  
765 repository.

## 766 **Author Contributions**

767 YS, KLB, AB and WAL conceived of the study, designed the study, and coordinated the study.  
768 YS and WD carried out the molecular lab work. YS and WAL conducted data analyses and  
769 drafted the manuscript; GJM helped interpreted the results regarding putative inversions. MC  
770 supervised the project. All authors commented the manuscript and gave final approval for  
771 publication.

## 772 **Conflict of Interest**

773 The authors declare that they have no conflict of interests.

774 **Figure 1.** (A) Map of the six study reaches along the Upper Mississippi River System, (B) key  
775 reproduction-related life history traits of the six study species, and (C) positions of the six study  
776 reaches in the environmental space of 20 variables using PCA biplot. See Table S1 for details of  
777 life history traits and Table S2 for details of environmental data. Use of fish images is permitted  
778 by Uland Thomas.

779 **Figure 2.** Manhattan plots depicting the genomic landscape of differentiation (F<sub>ST</sub>, corrected  
780  $F_{ST}$ ) across the genomes for the six study species. Species are ordered based on neutral  
781 population differentiation, with neutral global F<sub>ST</sub> values labeled next to the species name. At  
782 the top of each plot, genomic islands of differentiation identified using HMM after filtering are  
783 in blue, and islands located within the chromosomes showing clustered architecture are in purple.  
784 GEA outliers found within islands are in red, whereas those found outside of islands of genomic  
785 divergence are in orange. Reference genomes and alignment summary can be found in Table S3.

786 **Figure 3.** Principal component analyses using neutral SNPs only for the six study species. The  
787 percentage of variance explained by each principal component (PC) is labeled on the x- and y-  
788 axes.

789 **Figure 4.** Characterization of putative inversion on chromosome 9 in Emerald Shiner. (A) PCA  
790 based on SNPs within the putative inversion region. Three clusters identified using k-means  
791 clustering correspond to two homozygote groups (blue and red) and a heterozygote group  
792 (purple). The discreteness of the clustering was calculated by the proportion of the between-  
793 cluster sum of squares over the total using the R function *kmeans* in *adegenet*. (B) Observed  
794 individual heterozygosity in each PCA cluster. Significance was assessed using Wilcoxon tests  
795 with alpha level of 0.05. Note: \*\*\* = 0.001. (C) Genotype frequency distribution for putative  
796 inversion across six study reaches. Bars represent the proportion of individuals belonging to a  
797 PCA cluster. (D) and (E) are LD heatmaps for chromosome 9 using all individuals (D) and only  
798 individuals homozygous for the more common orientation (E).

799 **Figure 5.** Principal component analyses for Emerald Shiner using different sets of loci: (A) All  
800 aligned SNPs (3,348 SNPs); (B) Putative inversions on chromosome 6, 9 and 19 (228 SNPs); (C)  
801 After the removal of three putative inversions (3,120 SNPs). The percentage of variance  
802 explained by each principal component (PC) is labeled on the x- and y- axes.

803 **Figure 6.** Comparisons of corrected  $F_{ST}$  (F<sub>ST</sub>), heterozygosity ( $H_o$ ), absolute divergence ( $D_{xy}$ ),  
804 and LD ( $r^2$ ) between SNPs within the HMM islands (Island, red) and five combined random  
805 windows (Background, gray) on the corresponding chromosomes for chromosomes with  
806 clustered architecture, including on chromosome 7 and 17 in Freshwater Drum, chromosome 20  
807 and 28 in Channel Catfish, and chromosome 9 in Emerald Shiner. The average distance between  
808 pairs of SNPs within islands and random windows were labelled below the boxplots of LD  
809 values (column 4). Significance was assessed between islands and random windows using  
810 Wilcoxon tests with alpha level of 0.05. Note: \*\*\* = 0.001, \*\* = 0.01, \* = 0.05, NS = not  
811 significant. Only HMM islands with more than one SNP were included.

**A****B**

### Key life history traits

Nest spawner

Open substratum spawner

Spawning migration



Bullhead Minnow (*I. aestivalis*)



White sucker (*C. commersoni*)



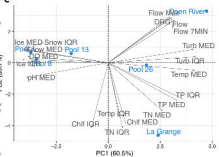
Rock Bass (*C. punctulatus*)



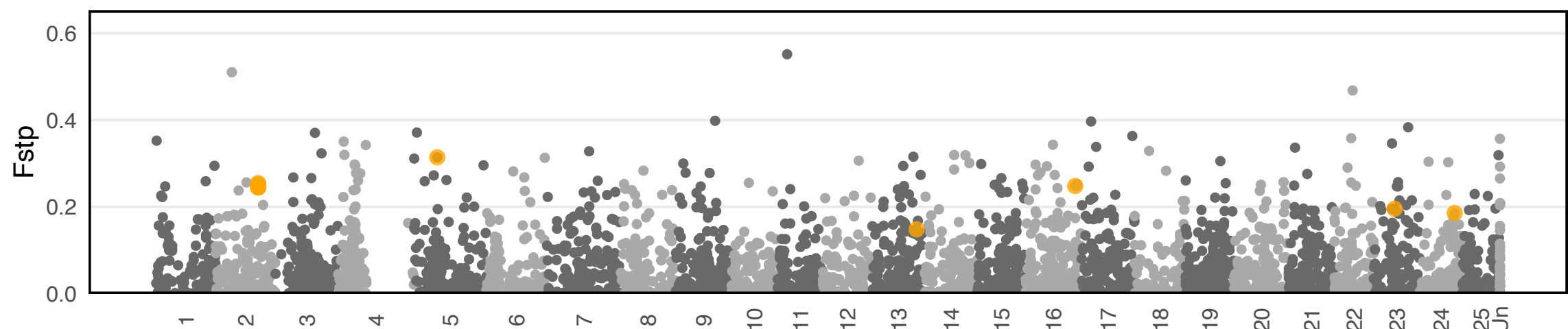
Gizzard Shiner (*C. heterodon*)



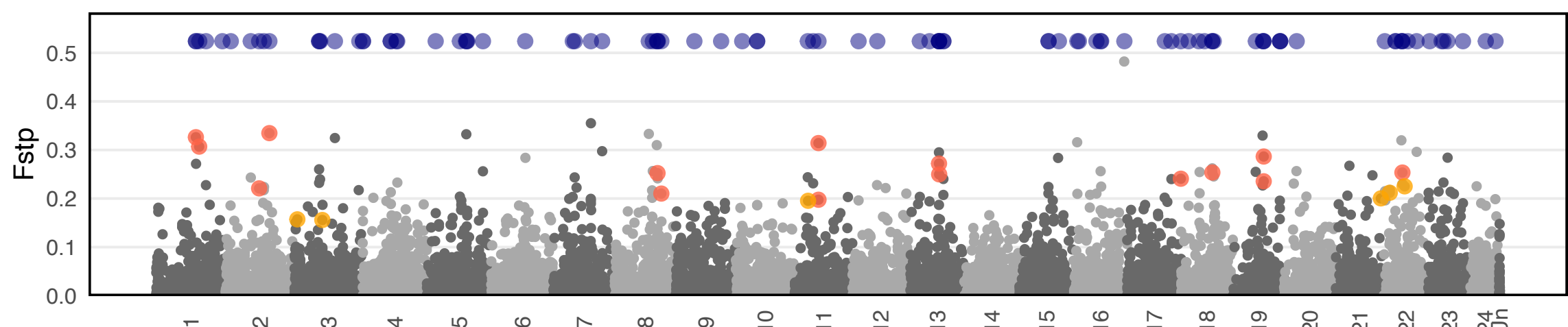
Bluegill (*L. macrochirus*)

**C**

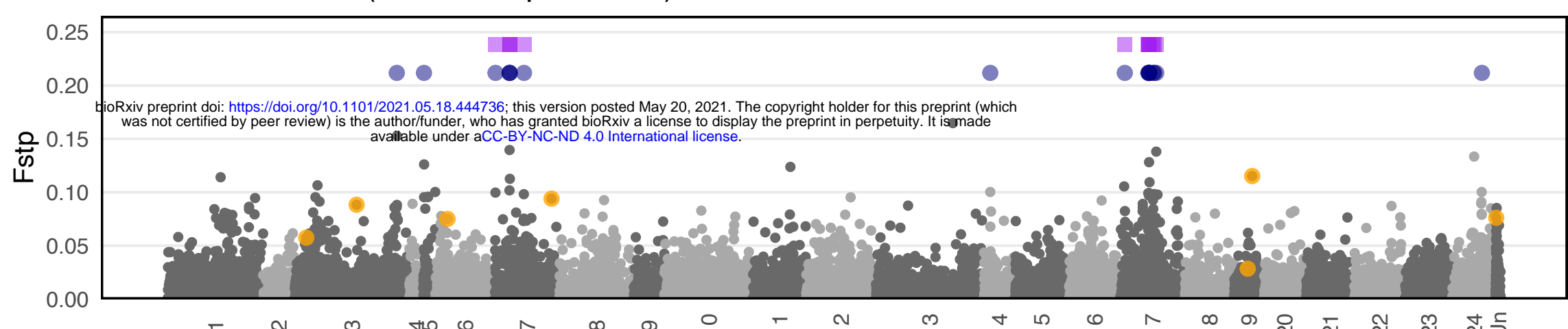
### Bullhead Minnow (Global Fst<sub>p</sub> = 0.072)



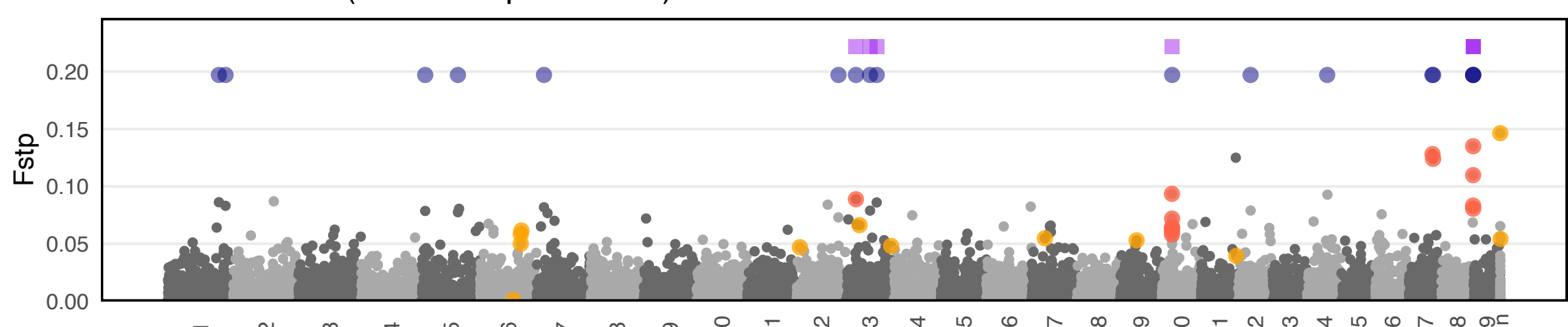
### Bluegill (Global Fst<sub>p</sub> = 0.0302)



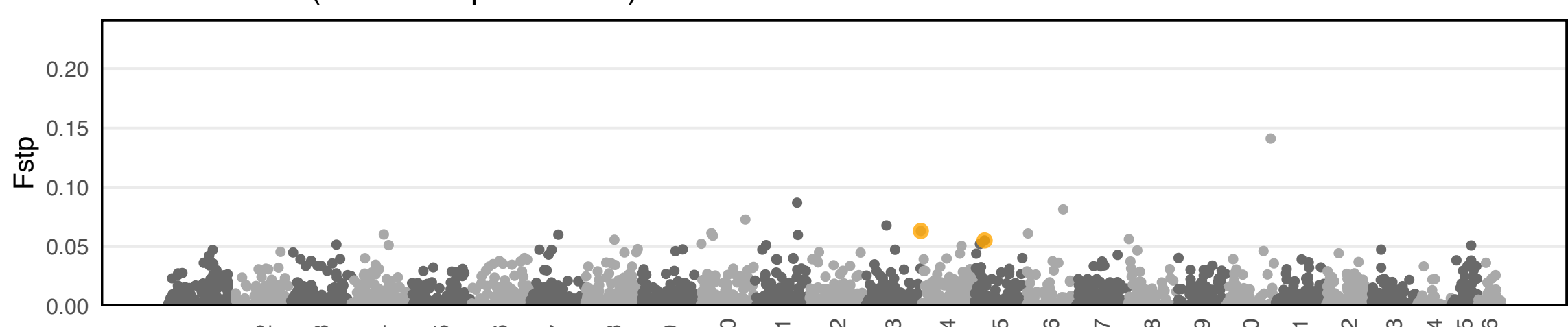
### Freshwater Drum (Global Fst<sub>p</sub> = 0.005)



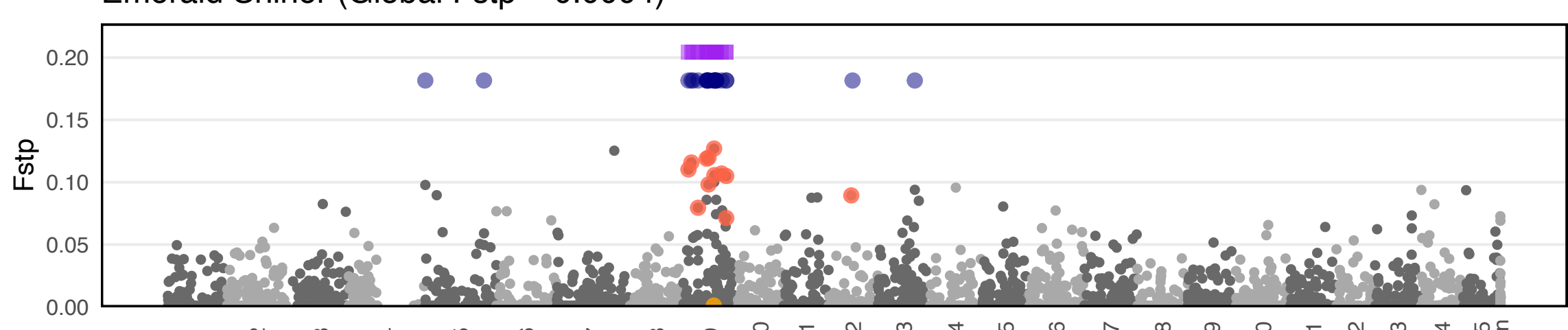
### Channel Catfish (Global Fst<sub>p</sub> = 0.0025)

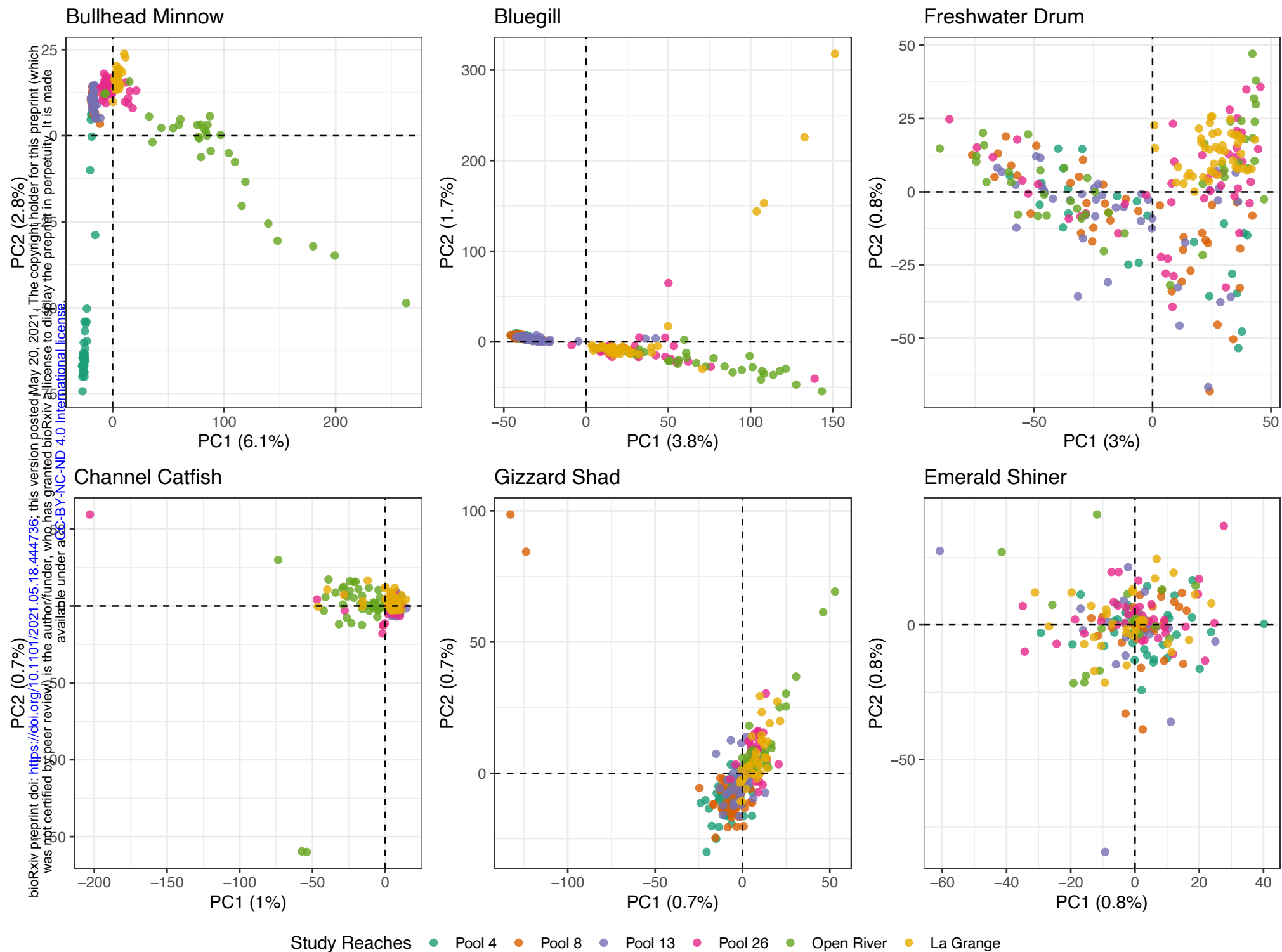


### Gizzard Shad (Global Fst<sub>p</sub> = 0.0024)

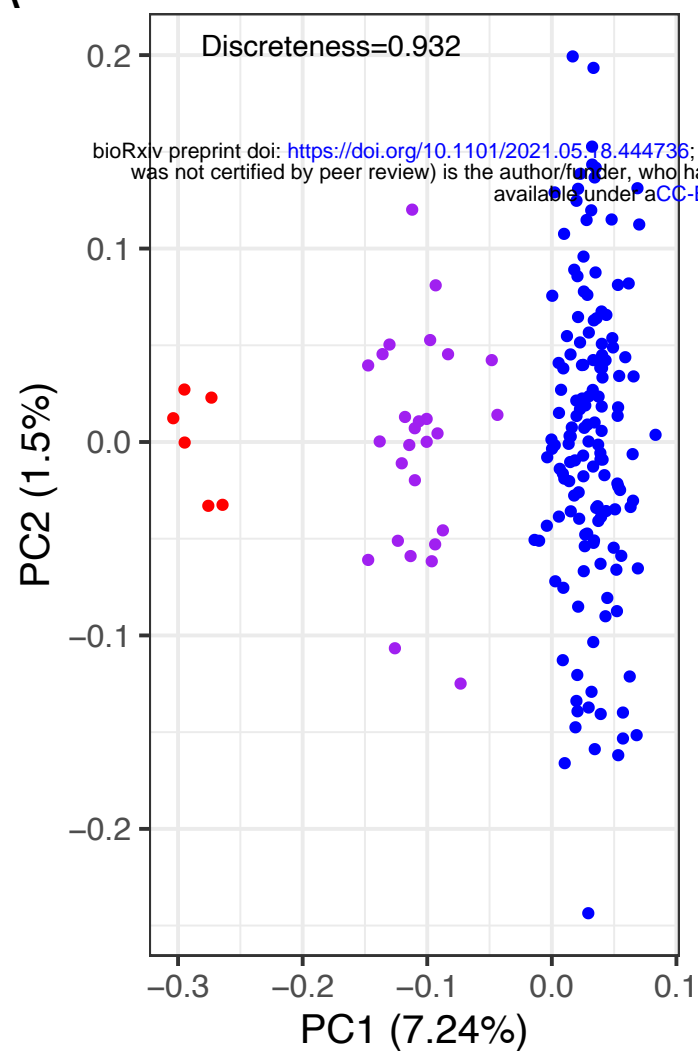


### Emerald Shiner (Global Fst<sub>p</sub> = 0.0004)

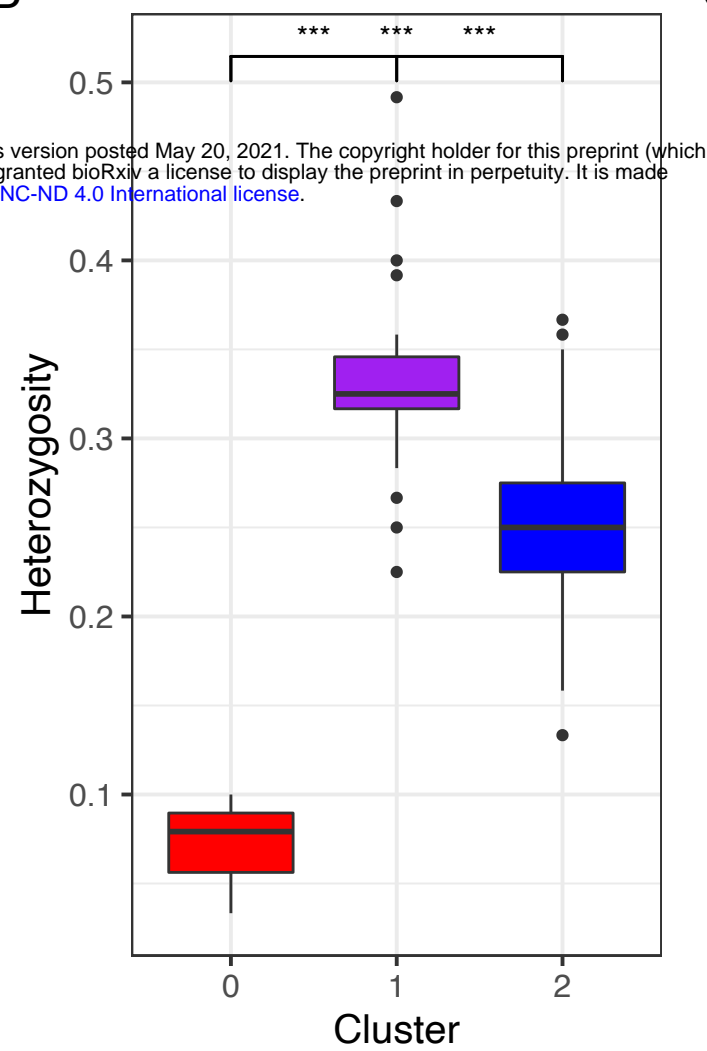




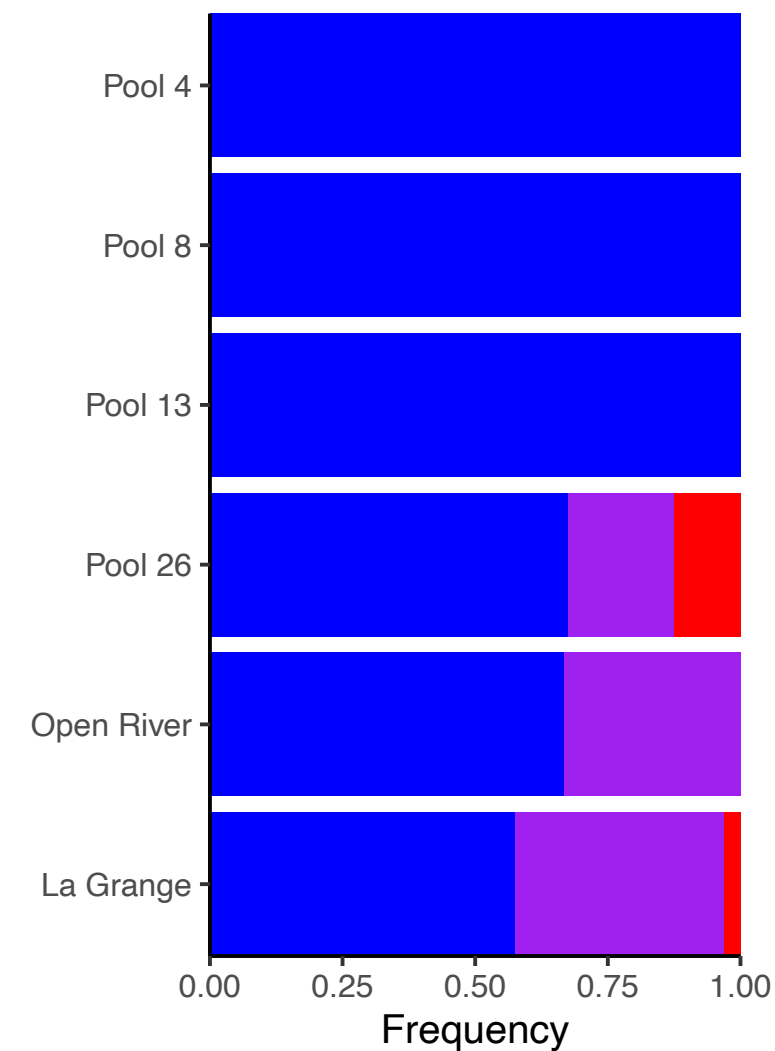
A



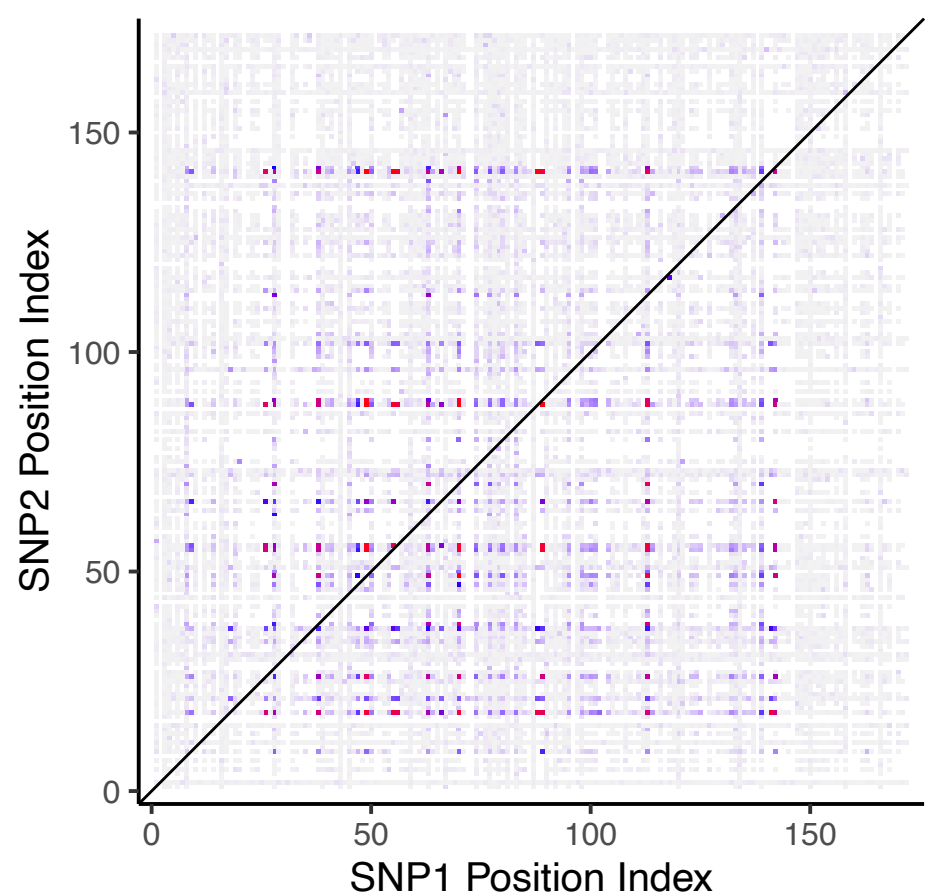
B



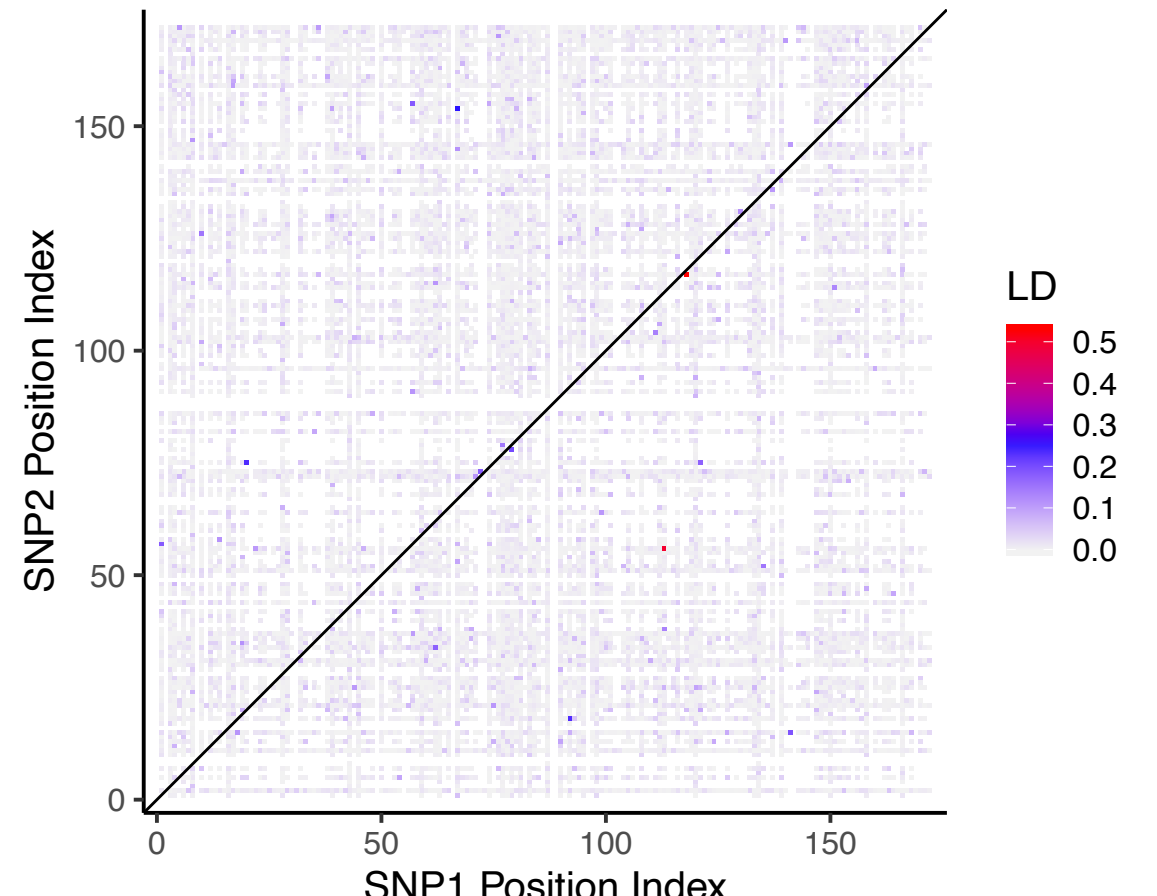
C



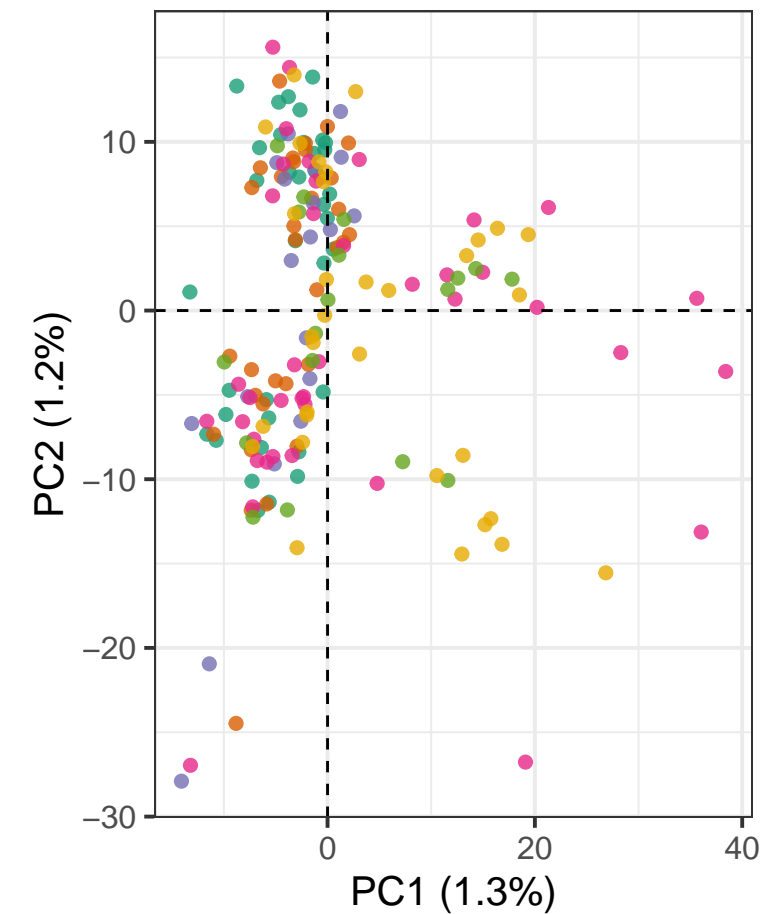
D



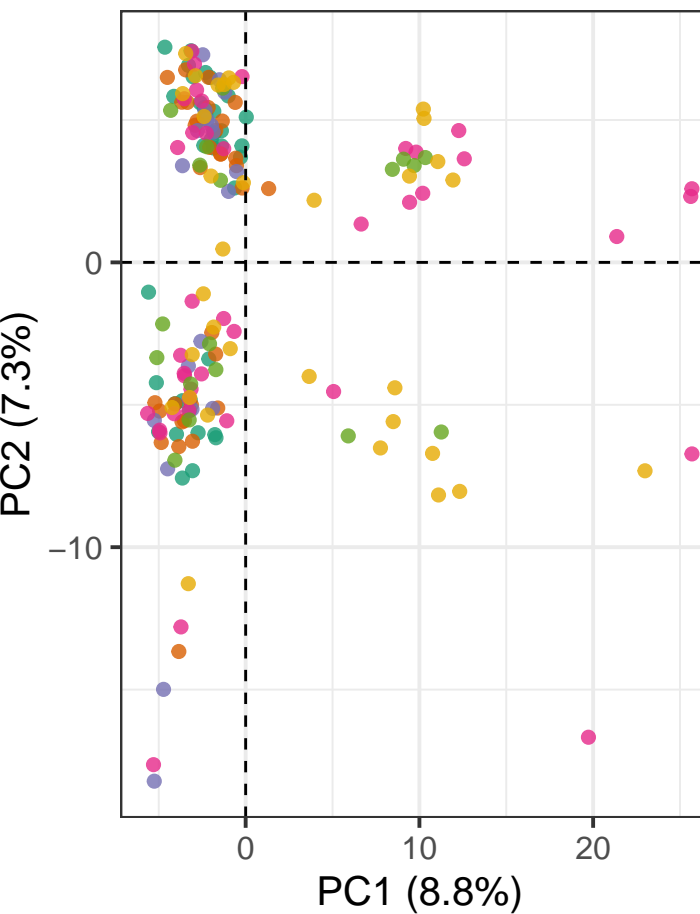
E



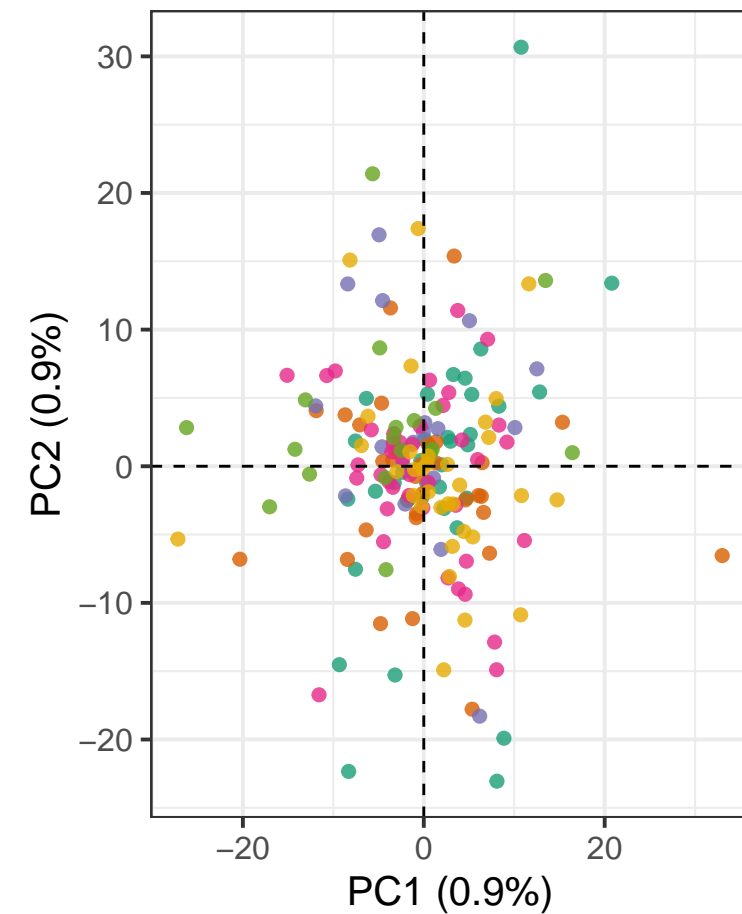
### All loci



### Three inversions

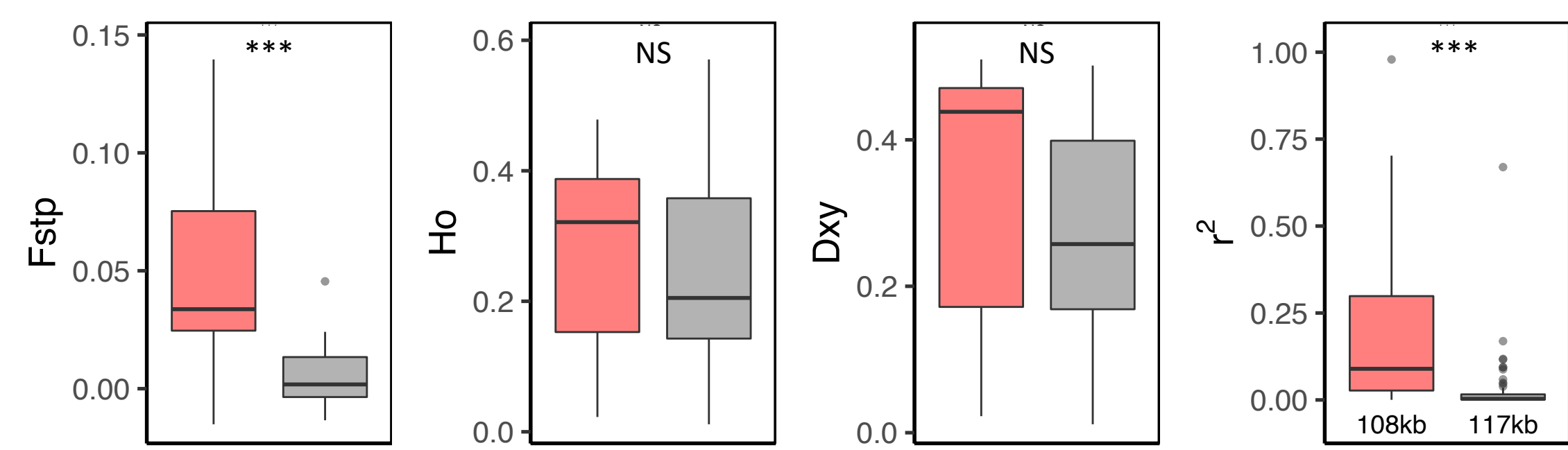


### No inversions

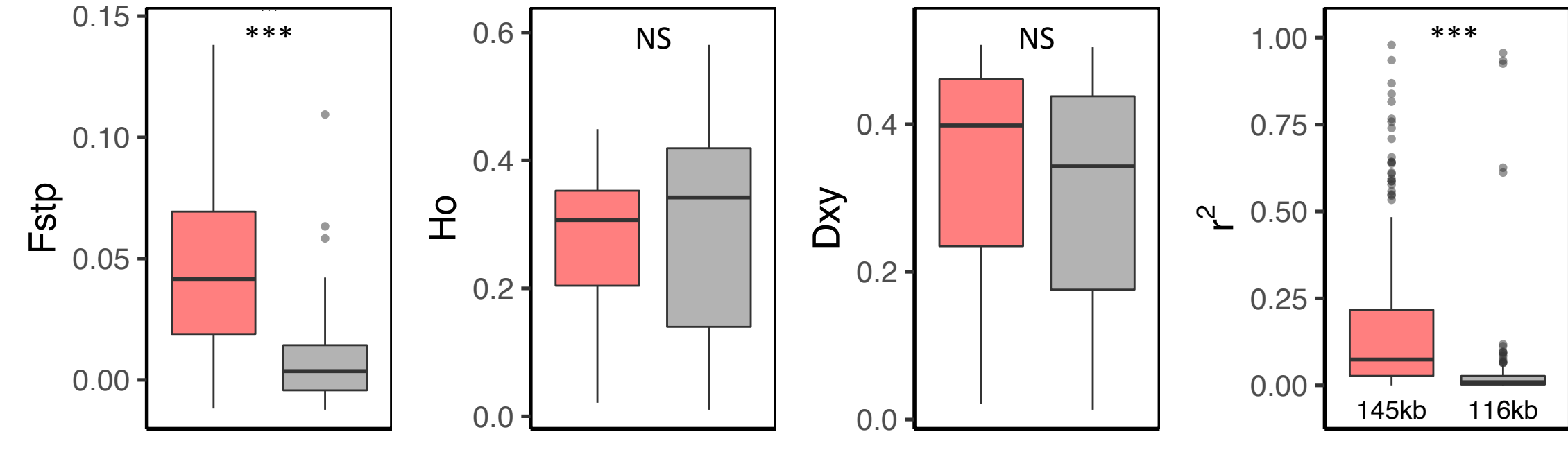


Study Reaches • Pool 4 • Pool 8 • Pool 13 • Pool 26 • Open River • La Grange

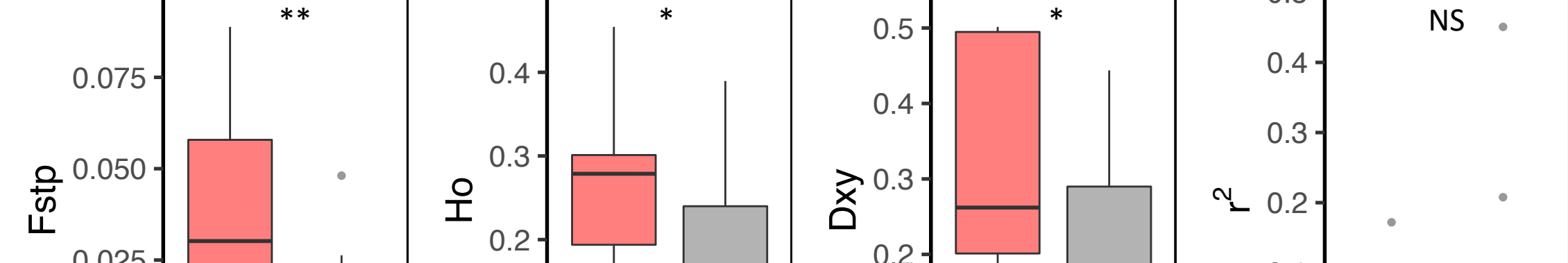
# Freshwater Drum Chromosome 7



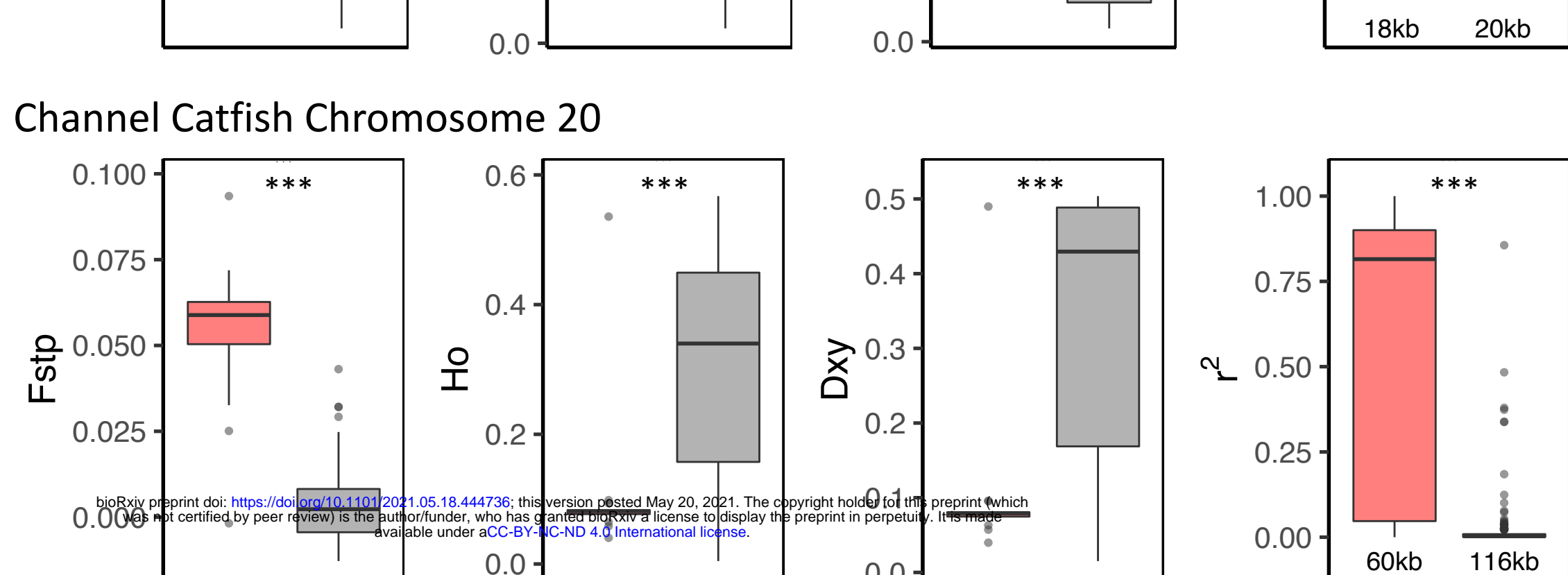
# Freshwater Drum Chromosome 17



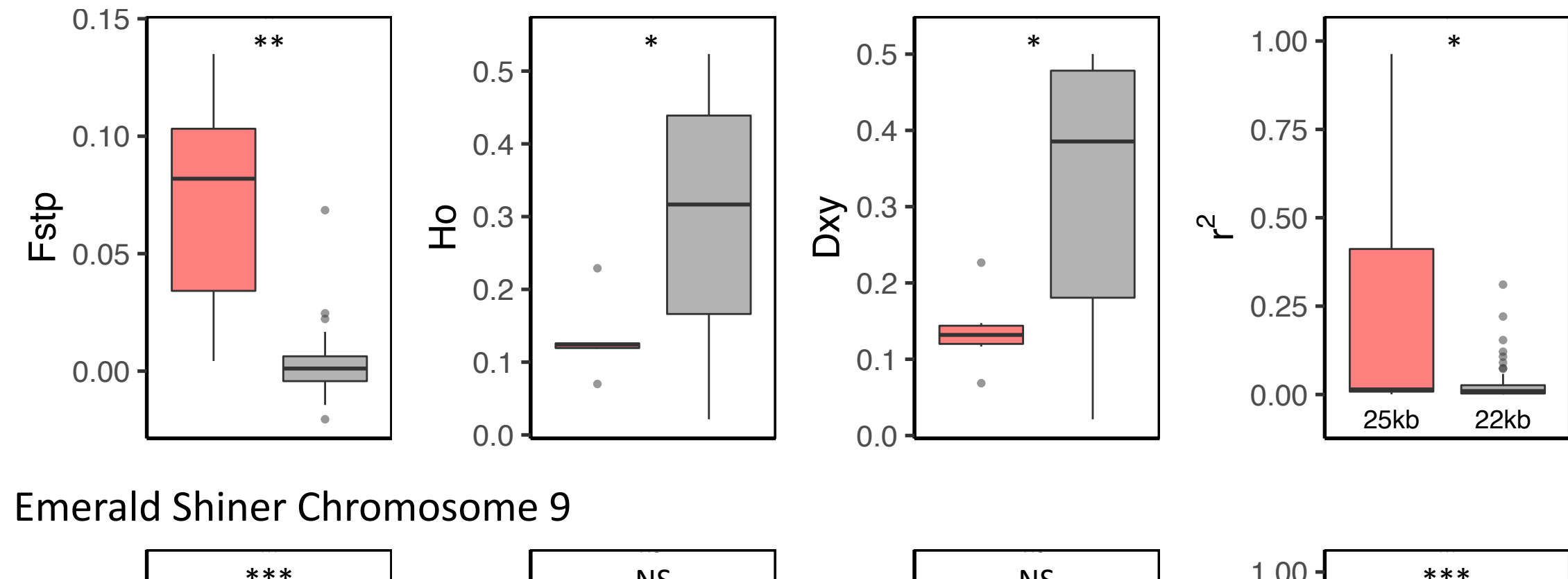
# Channel Catfish Chromosome 13



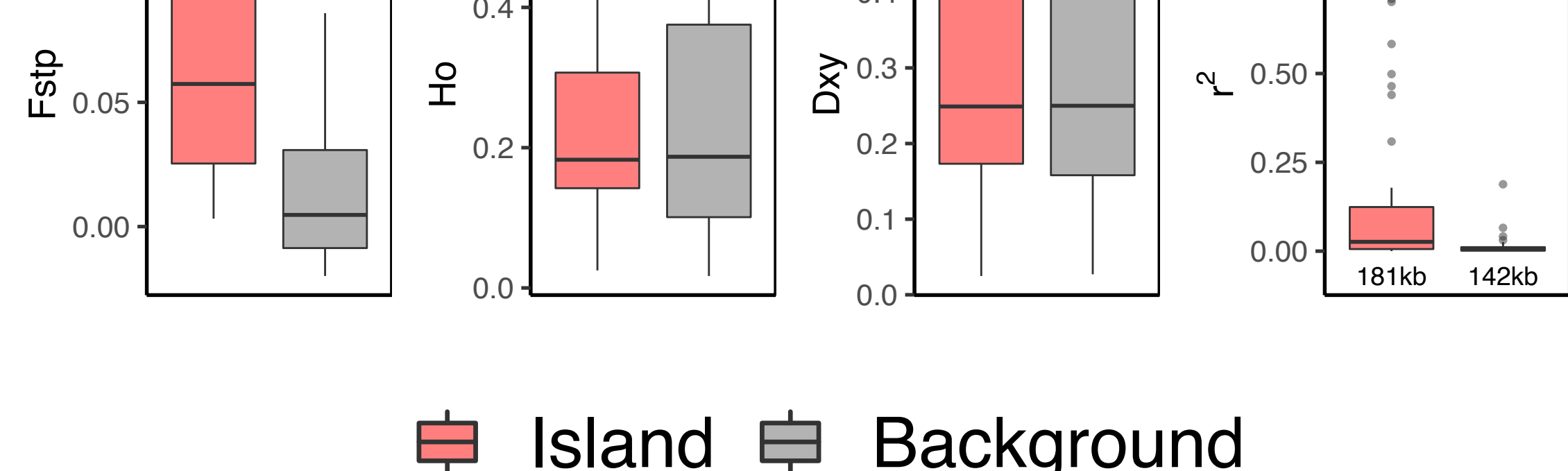
# Channel Catfish Chromosome 20



# Channel Catfish Chromosome 28



# Emerald Shiner Chromosome 9



■ Island ■ Background